J. Membrane Biol. 130, 63–82 (1992)

The Journal of
Membrane Biology

Rapid Ca^{2+} Extrusion Via the Na^+/Ca^{2+} Exchanger of the Human Platelet

Peter A. Valant, Philip N. Adjei, and Duncan H. Haynes
Department of Molecular and Cellular Pharmacology, University of Miami School of Medicine, Miami, Florida 33101

Summary. This communication reports the kinetics of the Na^+/Ca^{2+} exchanger and of the plasma membrane (*PM*) Ca^{2+} pump of the intact human platelet. The kinetic properties of these two systems were deduced by studying the rate of Ca^{2+} extrusion and its Na^+ dependence for concentrations of cytoplasmic free Ca^{2+} ($[Ca^{2+}]_{cyt}$) in the 1–10-μM range. The *PM* Ca^{2+}-ATPase was previously characterized (Johansson, J.S. Haynes, D.H. 1988. *J. Membrane Biol.* **104:**147–163) for $[Ca^{2+}]_{cyt} \leq 1.5$ μM with the fluorescent Ca^{2+} indicator quin2 (K_d = 115 nM). That study determined that the *PM* Ca^{2+} pump in the basal state has a V_{max} = 0.098 mM/min, a K_m = 80 nM and a Hill coefficient = 1.7. The present study extends the measurable range of $[Ca^{2+}]_{cyt}$ with the intracellular Ca^{2+} probe, rhod2 (K_d = 500 nM), which has almost a fivefold lower affinity for Ca^{2+}. An Appendix also describes the Mg^{2+} and pH dependence of the K_d and fluorescence characteristics of the commercially available dye, which is a mixture of two molecules. Rates of active Ca^{2+} extrusion were determined by two independent methods which gave good agreement: (i) by measuring Ca^{2+} extrusion into a Ca^{2+}-free medium (above citation) or (ii) by the newly developed "ionomycin short-circuit" method, which determines the ionomycin concentration necessary to short circuit the *PM* Ca^{2+} extrusion systems. Absolute rates of extrusion were determined by knowledge of how many Ca^{2+} ions are moved by ionomycin per minute. The major findings are as follows: (i) The exchanger is saturable with respect to Ca^{2+} with a K_m = 0.97 ± 0.31 μM and V_{max} = 1.0 ± 0.6 mM/min. (ii) At high $[Ca^{2+}]_{cyt}$, the exchanger works at a rate 10 times as large as the basal V_{max} of the *PM* Ca^{2+} extrusion pump. (iii) The exchanger can work in reverse after Na^+ loading of the cytoplasm by monensin. (iv) The *PM* Ca^{2+} extrusion pump is activated by exposure to $[Ca^{2+}]_{cyt} \geq 1.5$ μM for 20–50 sec. Activation raises the pump V_{max} to 1.6 ± 0.6 mM/min and the K_m to 0.55 ± 0.24 μM. (v) The Ca^{2+} buffering capacity of the cytoplasm is 3.6 mM in the 0.1 to 3 μM range of $[Ca^{2+}]_{cyt}$. In summary, the results show that the human platelet can extrude Ca^{2+} very rapidly at high $[Ca^{2+}]_{cyt}$. Both the Na^+/Ca^{2+} exchanger and Ca^{2+} pump activation may prevent inappropriate platelet activation by marginal stimuli.

Key Words Na^+/Ca^{2+} exchanger · plasmalemmal Ca^{2+}-Mg^{2+} ATPase · platelets, human · fluorescent Ca^{2+} indicators (rhod2 & quin2) · kinetics of Ca^{2+} extrusion · calmodulin activation

Introduction

Cytoplasmic Ca^{2+} activity ($[Ca^{2+}]_{cyt}$)[1] plays an important regulatory role in platelet function. Figure 1 is a schematic of the mechanisms involved in main-

[1] *Abbreviations:* cAMP, cyclic adenosine 3′,5′-monophosphate; cGMP, cyclic guanosine 3′,5,-monophosphate; Ca-CAM, calcium calmodulin; *DT*, dense tubules; *B*, intrinsic cytoplasmic Ca^{2+} binding sites; *R*, rhod2 or 5-(3,6-bis(dimethylamino)xanth-9-*yl*)-1-(2-amino-4-hydroxylphenoxy)-2-(2-amino-5-methylphenoxy)ethane-N,N,N′N′-tetraacetic acid; $[Ca^{2+}]_{cyt}$, cytoplasmic Ca^{2+} activity; quin2, 2-[[2-bis[(carboxymethyl)amino]-5-methylphenoxy]methyl]-6-methoxy-8-[bis(carboxymethyl)amino]quinoline; V or $V_{extrusion}$, true rate of Ca^{2+} extrusion; fura-2, 1-[2-(5-carboxyoxazol-2-*yl*)-6-aminobenzofuran-5-oxy]-2-(2′-amino-5′-methylphenoxy)-ethane-N,N,N′N′-tetraacetic acid; AM, acetoxymethyl ester; DMSO, dimethylsulfoxide; CTC, chlortetracycline; EGTA, ethyleneglycol-bis(β-aminoethyl ether) N,N,N,N′-tetraacetic acid; HEPES, 4-(2-hydroxyethyl)-1-piperazine ethanesulfonic acid; NMDG, N-methyl-D-glucamine; PIPES, 1,4-piperazine-bis-(ethanesulfonic acid); HPLC, high performance liquid chromatography; α_1, fraction of high-affinity rhod2 complexed with Ca^{2+}; *F*, the observed fluorescence; F_{min}, the minimal fluorescence observed in the absence of Ca^{2+}; F_{max}, the maximal fluorescence observed when the dye is saturated with Ca^{2+}; X_1, the fraction of high-affinity dye; $K_{d,1}$, dissociation constant of high-affinity dye; $K_{d,2}$, dissociation constant of the low-affinity dye; $-d\alpha_1/dt$, rate of Ca^{2+} removal from the rhod2-Ca complex; $-dF/dt$, the slope representing the absolute rate of fluorescence decrease in a progress curve; $\Delta F_{max} = (F_{max} - F_{min})_{cyt}$, difference between maximal and minimal fluorescence for cytoplasmic high-affinity form of rhod2; F_{50}, fluorescence of the high-affinity form of rhod2 for $[Ca^{2+}]_{cyt}$ = 50 nM; $[Ca^{2+}]_o$, external Ca^{2+} concentration; K_P, proportionality constant between the total number of Ca^{2+} ions moved and the change in high-affinity rhod2 complexation to Ca^2; $(d[Ca^{2+}]_{cyt,T})/dt$, rate of Ca^{2+} influx obtained with maximal levels of ionomycin; k_{leak}, rate constant for passive inward Ca^{2+} leakage; k_{iono}, rate constant for ionomycin-mediated Ca^{2+} influx; *T*, total; $[rhod2]_{cyt,T}$, total intracellular rhod2 concentration; $[quin2]_{cyt,T}$, total intracellular quin2 concentration; $[B]_T$, total cytoplasmic buffering capacity; $\Delta[Ca^{2+}]_{cyt,T}$, total number

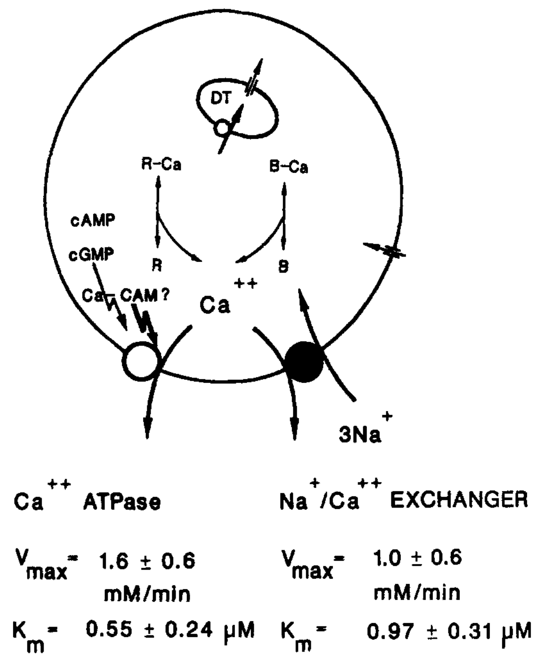

Fig. 1. A schematic (Johansson & Haynes, 1988) showing the two major processes responsible for the extrusion of Ca^{2+} across the plasma membrane, the Ca^{2+}-ATPase and the Na^+/Ca^{2+} exchanger. The activity of these is opposed by the inward passive leakage of Ca^{2+} across the plasmalemma. Both cAMP and cGMP stimulate the Ca^{2+}-ATPase (Johansson et al., 1992; Johansson & Haynes, 1992). Within the platelet the dense tubules (*DT*) are able to sequester cytoplasmic Ca^{2+} via a dense tubular Ca^{2+} pump. The activity of the latter is opposed by passive Ca^{2+} leakage from the dense tubules. The letter *B* denotes intrinsic cytoplasmic Ca^{2+} binding sites, while *R* denotes rhod2, the Ca^{2+}-sensitive fluorescent probe used to measure the cytoplasmic Ca^{2+} activity. The values of kinetic parameters shown are based on results obtained in the present study. Note that the values shown for the Ca^{2+} pump apply only to the activated state. Ca-CAM denotes the calcium-calmodulin complex.

of Ca^{2+} ions moved into the cytoplasm; $\Delta[\text{rhod2-Ca}]_{cyt,T}$, change in concentration of total intracellular high-affinity rhod2 complexed to Ca^{2+}; $\Delta[B\text{-Ca}]_T$, change in concentration of total cytoplasmic binding sites complexed to Ca^{2+}; $\Delta[\text{quin2}]_{cyt,T}$, change in concentration of total intracellular quin2 complexed to Ca^{2+}; $\Delta\alpha$, change in the degree of intracellular quin2 saturation; $\Delta\alpha_1$, change in degree of saturation of cytoplasmic high-affinity rhod2; $\Delta\alpha_1/\Delta t$, rate of change in degree of saturation of cytoplasmic high-affinity rhod2; V_{obs}, observed rate of Ca^{2+} removal from the rhod2-Ca complex; $V_{8.3\,\mu M}$, the rate of Ca^{2+} removal from the high-affinity rhod2-Ca complex at $[Ca^{2+}]_{cyt}$ = 8.3 μM; $\Delta\alpha/\Delta t$, rate of change in of the degree of quin2 saturation, α; $\Delta[Ca^{2+}]_{cytT}/\Delta t$, initial linear rate of ionomycin-mediated Ca^{2+} influx; EC_{50}, effective concentration giving a half-maximal effect; $[Na^+]_{cyt}$, cytoplasmic Na^+ activity; CAM, calmodulin; ACN, acetonitrile; and TFA, trifuloroacetic acid.

taining cytoplasmic Ca^{2+} homeostasis in the resting human platelet. The resting $[Ca^{2+}]_{cyt}$ is maintained by a balance between leakage of Ca^{2+} into the cytoplasm from the extracellular medium and its clearance from the cytoplasm by plasmalemmal extrusion mechanisms (Johansson & Hayes, 1988). In Fig. 1 these are shown as a Ca^{2+}-Mg^{2+} ATPase and a Na^+/Ca^{2+} exchanger. The dense tubular Ca^{2+} pump also responds to changes in $[Ca^{2+}]_{cyt}$ (Jy & Haynes, 1987). In the quiescent platelet, $[Ca^{2+}]_{cyt}$ determines the concentration of dense tubular Ca^{2+} and hence the amount of Ca^{2+} that can be released by activators of platelet aggregation (Jy & Haynes, 1987; Jy et al., 1987). The Na^+/Ca^{2+} exchanger has been previously identified and the kinetics of plasmalemmal Ca^{2+}-ATPase have been determined for values of $[Ca^{2+}]_{cyt} \leq 1.5$ μM (Johansson & Haynes, 1988). However, in that study the measurable range of $[Ca^{2+}]_{cyt}$ values was too low to reveal saturation kinetics of the Na^+/Ca^{2+} exchanger. This paper will focus on further characterization of the Na^+/Ca^{2+} exchanger at higher levels of $[Ca^{2+}]_{cyt}$ (i.e., 1–10 μM).

Previous *in situ* characterization of Ca^{2+} extrusion mechanisms in the human platelet was achieved by analysis of the extrusion process in quin2-overloaded platelets (Johansson & Haynes, 1988). In this study, the kinetic parameters of a saturable component identifiable with the plasmalemmal Ca^{2+}-Mg^{2+} ATPase were determined and the presence of a Na^+/Ca^{2+} exchanger was demonstrated. The Ca^{2+} dependence of the rate of extrusion, $V_{extrusion}$ was shown to conform to the equation:

$$V_{extrusion} = \frac{V_{max,1} \cdot [Ca^{2+}]_{cyt}^{1.7}}{K_{m,1}^{1.7} + [Ca^{2+}]_{cyt}^{1.7}} + V_{exchanger} \quad (1)$$

where the first term with a 1.7 power dependence on $[Ca^{2+}]_{cyt}$ refers to the Ca^{2+} ATPase pump (K_m = 0.08 μM). The exchanger, represented by the second term in Eq. (1) showed an apparently linear dependence on $[Ca^{2+}]_{cyt}$ in the 0.1–1.5-μM range ($K_m \geq 1$ μM). The Na^+/Ca^{2+} exchanger was identified by its Na^+ dependence, which became apparent for Ca^{2+} extrusion in the $[Ca^{2+}]_{cyt} \geq$ 400-nM range (Johansson & Haynes, 1988). However, further characterization of the Na^+/Ca^{2+} exchanger at values of $[Ca^{2+}]_{cyt} > 1.5$ μM was not possible because the quin2 signal, which has a K_d of 115 nM, saturated at values of $[Ca^{2+}]_{cyt}$ below the larger working range of the Na^+/Ca^{2+} exchanger.

The earliest evidence for the presence of a Na^+/Ca^{2+} exchanger in the human platelet was provided by Rengasamy, Soura and Feinberg (1987). These investigators showed that plasma membrane vesicles isolated from human platelets exhibited $^{45}Ca^{2+}$ uptake in exchange for intravesicular Na^+. They also demonstrated that Ca^{2+} efflux from Ca^{2+}-loaded vesicles is Na^+ dependent and that the process of Na^+/Ca^{2+} exchange is electrogenic. Moreover, they found that Ca^{2+}-dependence of the Na^+-dependent Ca^{2+} uptake by the vesicles displays saturation kinetics with a K_m of 22 μM. This was followed by our observation of a Na^+-dependent component of Ca^{2+} extrusion in intact platelets (Johansson & Haynes, 1988) as described in the preceding paragraph. Further confirmation of the presence of a Na^+/Ca^{2+} exchanger has been provided by Schaeffer and Blaustein (1989) with fura2-laden platelets. They showed that isosmolar substitution of external Na^+ by sucrose caused a significant rise in cytoplasmic free Ca^{2+}, indicating operation of the exchanger in the reverse. Conversely, partial restoration of external Na^+ to platelets suspended in Na^+-free media resulted in a significant and rapid drop in cytoplasmic Ca^{2+} activity. A finding similar to the first of these observations was made in our laboratory: Addition of monensin, an ionophore which allows Na^{2+} entry into the cell by catalyzing Na^+/H^+ exchange across the cell membrane, increases resting $[Ca^{2+}]_{cyt}$ (Johansson, 1990).

The present study uses the fluorescent Ca^{2+} probe, rhod2, to determine the *in situ* Ca^{2+} dependence of the Na^+/Ca^{2+} exchanger over the 1–10-μM range of $[Ca^{2+}]_{cyt}$ values. Since rhod2 has been reported to have a lower affinity for Ca^{2+} (K_d = 1 μM; Minta, Kao & Tsien, 1989), this range is higher than that accessible to quin2 (Johansson & Haynes, 1988). Thus, by using rhod2-laden platelets we have determined the relative contribution of the exchanger and the Ca^{2+} pump to the extrusion process. This was done by two methods: (i) a modification of the net Ca^{2+} extrusion protocol initially developed by Johansson and Haynes (1988) and (ii) the ionomycin short-circuit method, developed in the present paper.

The present study will show that the results based on these two approaches give similar values for the V_{max} and the K_m of the Na^+/Ca^{2+} exchanger. Evidence will also be presented showing that the plasmalemmal Ca^{2+}-ATPase is activated after prolonged exposure to high levels of $[Ca^{2+}]_{cyt}$.

Materials and Methods

Chemicals

Dimethylsulfoxide (DMSO) was from Aldrich Chemical, Milwaukee, WI. Rhod2/AM (cell permeant; lot numbers 8A, 8B, and 10A) and rhod2 (cell impermeant; lot numbers 8A and 10A) were obtained from Molecular Probes, Eugene, OR. Ionomycin was purchased from Calbiochem, San Diego, CA. Chlortetracycline (CTC), digitonin, ethyleneglycol-bis-(β-aminoethyl ether) N,N,N',N'-tetraacetic acid (EGTA), 4(2-hydroxyethyl)-1-piperazine ethanesulfonic acid (HEPES), N-methyl-D-glucamine (NMDG), 1,4-piperazine-bis-(ethanesulfonic acid) (PIPES), quin2/AM and quin2 were supplied by Sigma Chemical, St. Louis, MO. $CaCl_2$, KCl, NaCl, and $NaHCO_3$ were purchased from Mallinckrodt, Paris, KY.

Solutions

The Na^+ Tyrode used for platelet isolation, loading with dye and temporary storage had the following composition (in mM): 135 NaCl, 2.7 KCl, 0.36 NaH_2PO_4, 11.9 $NaHCO_3$, 25 HEPES, and 10 D-glucose. In all experimentation, the Na^+ Tyrode was modified by omission of $NaHCO_3$ and its replacement by equimolar NaCl to give 146.9 mM NaCl.

Sodium-free media were prepared by isosmolar substitution of NMDGH-Cl for NaCl. All the media were titrated to the desired pH by the addition of HCl, NaOH, KOH, or NMDG. Stock solutions of rhod2/AM were prepared in DMSO. The concentration of DMSO during preincubation of platelets with 12 μM rhod2/AM was 0.6% (vol/vol). Stock solutions of ionomycin were prepared in ethanol.

Platelet Isolation

Platelets were isolated as previously described (Johansson & Haynes, 1988) with the following modification: the HEPES concentration of the Na^+ Tyrode used in platelet isolation was increased from 2.5 to 25 mM to improve its pH buffering capacity.

Fluorometry

The instruments and techniques used in fluorescence measurements have been previously described (Johansson & Haynes, 1988). For measurements of rhod2 fluorescence, the excitation wavelength was 553 nm and emission wavelength was 576 nm, with excitation and emission slits set at a width of 12 nm.

Rhod2 Loading

Suspensions of washed platelets (2 × 10^8 platelets/ml) were preincubated with rhod2/AM for 90 min at room temperature. The usual preincubation concentration of rhod2/AM was 12 μM. After the end of the preincubation interval, the platelet suspensions were then centrifuged at 400 × *g* and the pellets resuspended in an aliquot of Na^+ Tyrode at pH 7.35. The suspension was stored in the dark at room temperature, and its platelet concentration was determined turbidimetrically with periodic calibrations against a Coulter counter (Johansson & Haynes, 1988). Aliquots (40–100 μl) of the suspension were then introduced into various media after pre-equilibration of the latter to 37°C. The final volume was 2.0 ml, yielding a final concentration of 1.6 × 10^7 platelets/ml.

Preincubation of platelets with 12 μM rhod2/AM gave concentrations ranging between 0.05 and 0.5 mmol/liter cell volume. The intracellular concentration was determined as previously described for quin2 (Johansson & Haynes, 1988).

Characteristics of Rhod2 as a Ca^{2+} Indicator

Fluorometric Ca^{2+} titrations of the free form of the dye in vitro and of the product of rhod2/AM hydrolysis revealed the presence of two binding phenomena for Ca^{2+}, one with a high affinity for Ca^{2+} ($K_d \approx 0.5$ μM) and the other with a lower affinity ($K_d \approx 0.5$ mM). High performance liquid chromatography (HPLC) of rhod2 revealed that the commercially available product was a mixture of at least three components. (The determination of binding constants and HPLC analysis are described in greater detail in the Appendix). The fluorescence for a dye that has two affinities for Ca^{2+} is given by the following equation:

$$F = F_{min} + (F_{max} - F_{min}) \cdot \frac{X_1 \cdot [Ca^{2+}]}{K_{d,1} + [Ca^{2+}]} + \frac{(1 - X_1) \cdot [Ca^{2+}]}{K_{d,2} + [Ca^{2+}]} \quad (2)$$

where F is the observed fluorescence, F_{min} is the minimal fluorescence observed in the absence of Ca^{2+}, F_{max} is the maximal fluorescence observed when the dye is saturated with Ca^{2+}, X_1 is the fraction of dye in the high-affinity form, $K_{d,1}$ (500 nM) is its dissociation constant, and $(1 - X_1)$ and $K_{d,2}$ (0.5 mM) are the corresponding values for the low-affinity form. The value of X_1 is *ca.* 0.20. Ca^{2+} titrations show that the above value of X_1 applies to the free acid form of rhod2 in vitro, to the product of rhod2/AM hydrolysis in platelet lysates, and to dye trapped in the intracellular compartment (*cf.* Table A1 in Appendix). Thus, the total intracellular concentration of high-affinity rhod2 ($[rhod2]_{cyt,T}$) was calculated as 20% of the total dye concentration. It is implicit in this calculation that the quantum yields of both high- and low-affinity forms are equal.

Determination of Cytoplasmic Free Ca^{2+} with Rhod2

The cytoplasmic free Ca^{2+} ($[Ca^{2+}]_{cyt}$) was determined by the procedure given for quin2 by Tsien, Pozzan and Rink (1982*a*), after modification to take into account the following: First, a rather high rate of leakage necessitated corrections for the amount of dye in the external medium. This was determined from EGTA and Ca^{2+} jumps as described in the net Ca^{2+} extrusion protocol below. Second, the dye has two dissociation constants for Ca^{2+}, $K_{d,1} = 500$ nM and $K_{d,2} \approx 0.5$ mM. This necessitated the use of Eq. (2) for the extracellular compartment. In practice we found that $[Ca^{2+}]_{cyt}$ never reached levels sufficient for the low-affinity form of the dye to contribute significantly to the measured fluorescence. Thus, the following equation was adequate for calculating values of $[Ca^{2+}]_{cyt}$:

$$[Ca^{2+}]_{cyt} = K_{d,1} \cdot [\alpha_1/(1 - \alpha_1)] \quad (3)$$

where α_1 is the degree of complexation of the intracellular high-affinity form determined as

$$\alpha_1 = (F - F_{min})_{cyt}/(X_1 \cdot (F_{max} - F_{min})_{cyt}). \quad (4)$$

Here F is the measured fluorescence and X_1 is the fraction of high-affinity dye as defined in Eq. (2). In all determinations of $[Ca^{2+}]_{cyt}$ the value for $K_{d,1}$ was taken as 500 nM. This was based on our studies of the K_d for Ca^{2+} as a function of pH and $[Mg^{2+}]$ (*cf.* Appendix).

Because the leakage of dye into the external medium was a continuous process, attempts to remove the external dye by further washing would have yielded limited success. Moreover, manipulations that increased $[Ca^{2+}]_{cyt}$ accelerated the rate of dye loss. The Appendix shows that the two forms of the dye do not differ in their rate of leakage from the cytoplasmic compartment.

Study of the Na^+/Ca^{2+} Exchanger by the Net Ca^{2+} Extrusion Protocol (Method I)

Figure 2 illustrates the series of manipulations performed in a typical experiment to obtain progress curves of net Ca^{2+} extrusion from rhod2-laden platelets. As indicated by schematics shown in the figure, the protocol entails addition of external Ca^{2+} and ionomycin to increase $[Ca^{2+}]_{cyt}$ to about 10 μM. This is followed by the addition of EGTA to remove external Ca^{2+}. The resulting time-resolved decrease in fluorescence reflects the progress of unopposed active Ca^{2+} extrusion from the cytoplasm. On the extreme right, center and extreme left of the figure, the instantaneous changes in fluorescence seen upon addition of EGTA or external Ca^{2+} allow quantitation of the amount of external rhod2 that has leaked from the platelet.

The different steps of the protocol will now be described in sequence. The first addition of EGTA reduces the external $[Ca^{2+}]$ to zero. The next Ca^{2+} addition raises $[Ca^{2+}]_{ext}$ to 10 μM and thus saturates the external high-affinity form of the dye. The subsequent addition of 2.0 mM Ca^{2+} nearly saturates the external low-affinity form of the dye. The addition of ionomycin results in rapid Ca^{2+} influx resulting in the time-resolved increase in fluorescence. The latter levels off within 30–50 sec, indicating saturation of the cytoplasmic high-affinity form of rhod2. The addition of 1.99 mM EGTA lowers $[Ca^{2+}]_{ext}$ to *ca.* 10 μM and halts further Ca^{2+} influx. The resulting instantaneous decline in fluorescence reflects external low-affinity form. The subsequent time-resolved decrease in fluorescence represents the progress curve of extrusion. The progress curve flattens out at a $[Ca^{2+}]_{cyt}$ of about 50 nM. The instantaneous downward changes upon further EGTA additions reflect external high-affinity form.

It should be noted that in all experimentation involving chelation of Ca^{2+} by EGTA, the pH of the EGTA stock was preadjusted with sufficient base to prevent a pH change resulting from EGTA-Ca^{2+} complexation.

Inspection of Fig. 2 shows that exposure of platelets to high Ca^{2+} causes extra leakage of the low- and high-affinity forms of the dye. This is revealed by the larger amplitude of instantaneous fluorescence changes on the right-hand side (after ionomycin addition) than on the left-hand side of the figure. The extent of this leakage increases with length of the exposure to high levels of cytoplasmic Ca^{2+} and with magnitude of the rise in $[Ca^{2+}]_{cyt}$. Experiments which are described in more detail in the Appendix indicate the presence of a third form of the dye which is Ca^{2+} insensitive (probably unhydrolyzed rhod2/AM). Its release into the external medium is also increased by high $[Ca^{2+}]_{cyt}$. After its release, its contribution to measured fluorescence is 3–12% of $(F_{max} - F_{min})_{cyt}$.

Analysis of Progress Curves Obtained by the Net Extrusion Protocol

The kinetics of extrusion is analyzed by measuring the slopes (Fig. 2) which represent the absolute rates of fluorescence decrease ($-dF/dt$). The latter are then converted into rates of Ca^{2+}

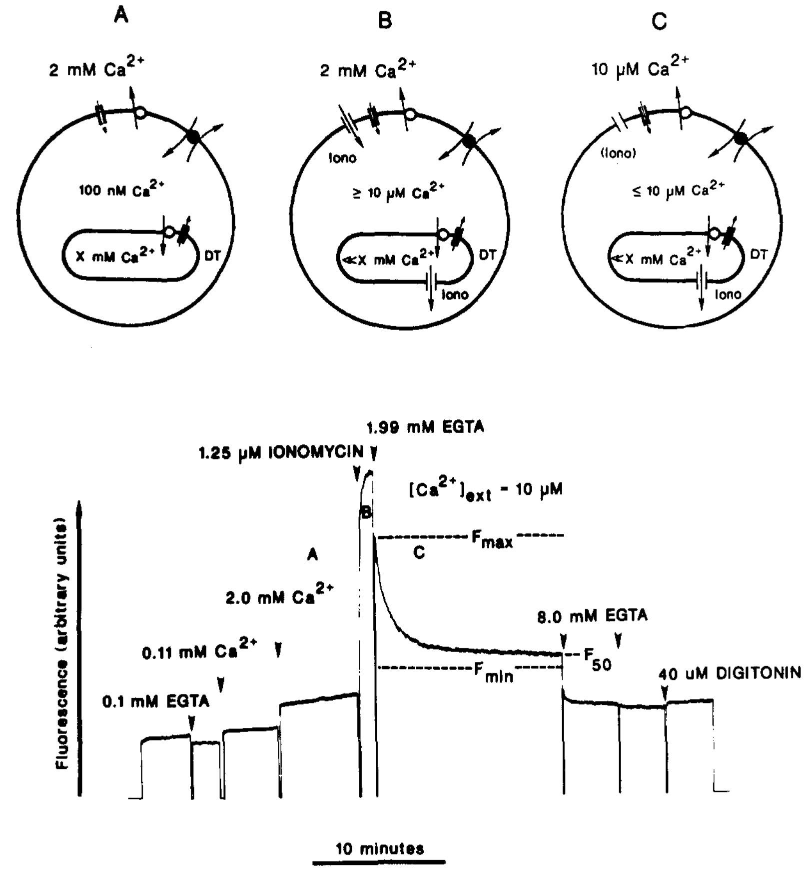

Fig. 2. Protocol used for measuring rates of active net Ca^{2+} extrusion with accompanying schematics (Method I). The amount of EGTA added after the ionomycin peak was such that $[Ca^{2+}]/[EGTA]$ ratio was 2.00/1.99 mM. This ratio yields an external free-Ca^{2+} concentration of about 10 μM. Dropping the $[Ca^{2+}]_{ext}$ to 10 μM eliminates the extracellular contribution of the low-affinity form but guarantees saturation of the extracellular high-affinity form. The latter condition is of particular advantage, since it ensures against the possibility that any extra leakage which might occur during the Ca^{2+} extrusion process will not be counted as Ca^{2+} extrusion. The term F_{50} refers to the fluorescence corresponding to this value of $[Ca^{2+}]_{cyst}$. Since 50 nM Ca^{2+} represents 10% of the K_d for Ca^{2+}, $\Delta F_{max} = 1.1 \cdot (F_{max} - F_{50})_{cyt}$. Abbreviations are defined as follows: Iono: ionomycin; *DT*: dense tubules.

removal from the rhod2-Ca complex $(-d\alpha_l/dt)$, which are given by:

$$(-d\alpha_l/dt) = (-dF/dt)/(X_1 \cdot (F_{max} - F_{min})_{cyt}). \quad (5)$$

Conversion of these rates into absolute rates was achieved by a calibration procedure which will be described below.

Calibration of Rhod2 Fluorescence Against That Measured in the Quin2-Overloaded Condition

The calibration method expands upon previous use of ionomycin as a quantitative tool (Johansson & Haynes, 1988). In the latter study, the kinetics of ionomycin-mediated Ca^{2+} influx into quin2-overloaded platelets was determined over a wide range of values of external Ca^{2+} concentration ($[Ca^{2+}]_o$) at a constant ionomycin concentration (100 nM). In the present study, $[Ca^{2+}]_o$ was kept constant and the ionomycin concentration varied to achieve different rates of Ca^{2+} influx. High ionomycin concentrations allowed determination of the proportionality constant (K_P) between the total number of Ca^{2+} ions moved ($\Delta[Ca^{2+}]_{cyt,T}$) and the corresponding change in degree of rhod2 complexation ($\Delta\alpha_l$). Knowledge of K_P allows determination of absolute number of Ca^{2+} ions moved and of the cytoplasmic buffering capacity. Determination of K_P required parallel experimentation with quin2-overloaded platelets, as will be shown below. Low concentrations of ionomycin (used on rhod2-laden platelets) allowed determination of kinetics of Ca^{2+} extrusion by an independent method (Method II), which will be described in the next subsection.

When varied concentrations of ionomycin are added to platelets in the presence of constant $[Ca^{2+}]_o$, the absolute rate of Ca^{2+} influx, (mmol Ca^{2+}/liter cell vol/min), is given by:

$$(d[Ca^{2+}]_{cyt,T})/dt = k_{leak} \cdot [Ca^{2+}]_o + (k_{iono} \cdot [Ca^{2+}]_o \cdot [\text{ionomycin}]) - V_{extrusion} \quad (6)$$

where $(d[Ca^{2+}]_{cyt,T})/dt$ is the rate of Ca^{2+} influx, k_{leak} and k_{iono}[2] are the rate constants for passive inward leakage through a Cd^{2+}-sensitive, verapamil-insensitive channel (Jy & Haynes, 1987) and for ionomycin-mediated Ca^{2+} influx, respectively. The rate of extrusion, $V_{extrusion}$ is a function of $[Ca^{2+}]_{cyt}$ as defined by Eq. (1) (*cf.* Introduction). The subscript T denotes total, and $[Ca^{2+}]_o$ is the external Ca^{2+} concentration.

When the ionomycin concentration is very high (≥ 1 μM), the initial rate of ionomycin-facilitated Ca^{2+} influx is so large that

[2] The Ca^{2+} dependence of the rate of ionomycin-mediated Ca^{2+} influx displays saturation kinetics with a K_m for Ca^{2+} of 7.7 mM (Johansson & Haynes, 1988). However, when the $[Ca^{2+}]_o$ is maintained constant at 2 mM, the dependence becomes a linear function of $[Ca^{2+}]_o$ as shown above. In the present study k_{iono} was found to be 4.4-fold higher than previously reported (Johansson & Haynes, 1988). We believe the higher value is more reliable. The turnover number for ionomycin is 40 mM Ca^{2+} per μmol ionomycin per min.

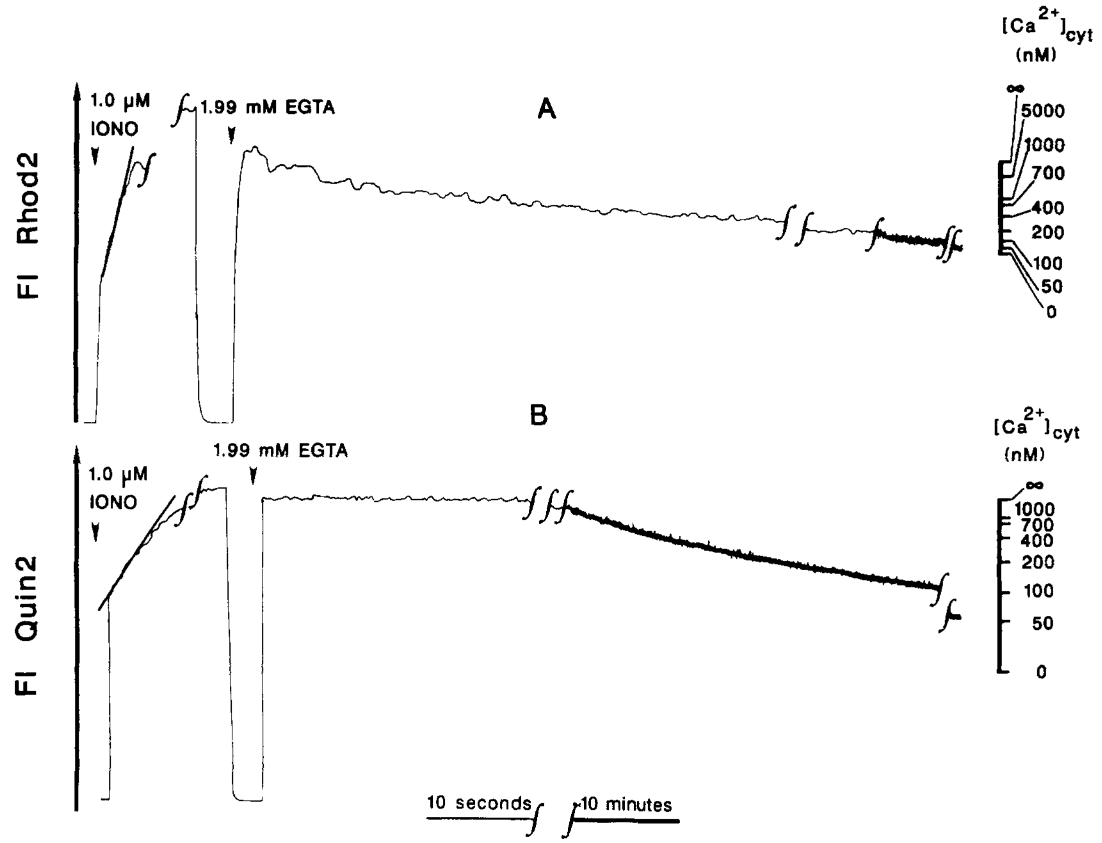

Fig. 3. Comparison of rates of Ca^{2+} influx and extrusion in rhod2-laden *vs.* quin2-overloaded platelets. Two experiments done with platelets from the same individual and performed under identical conditions are shown. (*A*) An experiment done with platelets overloaded with quin2 (preincubated with 20 μM quin2/AM; $[\text{quin2}]_{cyt}$ = 9.7 mM; exposure to 2 mM Ca^{2+} plus ionomycin lasted 42 sec). (*B*) A parallel experiment done with rhod2-laden platelets (preincubated with 12 μM rhod2/AM; $[\text{rhod2}]_{cyt}$ = 0.41 mM; exposure to 2 mM Ca^{2+} plus ionomycin lasted 38 sec). The slope of the initial rise in fluorescence immediately after ionomycin addition is used to calculate ($\Delta\alpha/\Delta t$), as defined in Eq. (13) after division of both sides by Δt (*cf.* Materials and Methods). The figure also compares the apparent Ca^{2+} extrusion rates in rhod2-laden *vs.* quin2-overloaded platelets. The vertical traces represent opening or closing of the shutter. The initial curvature at the end of these traces reflects the time constant for the response of the chart recorder. Ionomycin additions were made 1 sec prior to opening of the shutter. At the time of ionomycin addition $[Ca^{2+}]_o$ was 2.0 mM.

the first term (passive inward leak) and $V_{extrusion}$ can be neglected. Since both $[Ca^{2+}]_o$ and the ionomycin concentration are known, measurement of $(d[Ca^{2+}]_{cyt,T})/dt$ by the calibration method described below allows determination of the rate constant, k_{iono}.

Figure 3 (left-hand portion) shows a typical calibration used in the present study. Fluorescence changes observed in rhod2-laden platelets were compared with those observed in quin2-overloaded platelets, when both groups were exposed to 1 μM ionomycin in the presence of 2 mM external Ca^{2+}. This was done in parallel experiments performed under identical conditions. The concentration of ionophore was sufficient to overwhelm the Ca^{2+} extrusion systems (*cf.* Johansson & Haynes, 1988; Johansson, Neid & Haynes, 1992), such that the initial linear phase of Ca^{2+} influx was observed when unopposed. Though ionomycin moves an identical number of Ca^{2+} ions per liter cell volume per minute in each group of platelets, the linear rate of rise in fluorescence is steeper in rhod2-laden than in quin2-overloaded platelets. This difference reflects a much lower (*ca.* 20-fold) total intracellular concentration of rhod2 ($[\text{rhod2}]_{cyt,T}$) than of quin2 ($[\text{quin2}]_{cyt,T}$). As a result, rhod2 buffers the influxing Ca^{2+} less effectively. In rhod2-laden platelets, the highest $[\text{rhod2}]_{cyt,T}$ that can be achieved is about 0.5 mM. This concentration is less than the previously determined cytoplasmic buffering capacity ($[B]_T$) of 0.73 mM (Johansson & Haynes, 1988).

The total number of Ca^{2+} ions moved ($\Delta[Ca^{2+}]_{cyt,T}$) during the linear phase of Ca^{2+} influx in rhod2-laden platelets is given by (Johansson & Haynes, 1988):

$$\Delta[Ca^{2+}]_{cyt,T} = \Delta[\text{rhod2-Ca}]_{cyt,T} + \Delta[B\text{-Ca}]_T \quad (7)$$

where, $\Delta[\text{rhod2-Ca}]_{cyt,T}$ is the change in total intracellular concentration of the rhod2-Ca^{2+} complex and $\Delta[B\text{-Ca}]_T$ is the change in total Ca^{2+} concentration bound to cytoplasmic binding sites ($[B]_T$). Since it is known that the ionomycin-mediated $\Delta[Ca^{2+}]_{cyt,T}/\Delta t$ is initially constant (*cf.* Eq. (6)), and it is shown in Fig. 3 that $\Delta[\text{rhod2-Ca}]_{cyt,T}/\Delta t$ is constant (the corresponding rate of fluorescence change is linear), $\Delta[Ca^{2+}]_{cyt,T}$ and $\Delta[\text{rhod2-Ca}]_{cyt,T}$ in Eq. (7) are proportional. Thus, Eq. (7) can be rearranged, so that

$$\Delta[Ca^{2+}]_{cyt,T} = \Delta[\text{rhod2-Ca}]_{cyt,T} \cdot K_P \quad (8)$$

where K_P, is the proportionality constant described above. K_P is given by:

$$K_P = 1 + \frac{\Delta[B\text{-Ca}]_T}{\Delta[\text{rhod2-Ca}]_{\text{cyt},T}}. \tag{9}$$

Determination of K_P requires performance of a parallel quin2-overload experiment, as will be explained below.

In quin2-overloaded platelets, the equation corresponding to Eq. (7) can be written as:

$$\Delta[Ca^{2+}]_{\text{cyt},T} = \Delta[\text{quin2-Ca}]_{\text{cyt},T}. \tag{10}$$

Here the right-hand term represents the change in the number of Ca^{2+} ions complexed to quin2. The second term defined in Eq. (7) can be neglected because the intracellular quin2 concentration ($[\text{quin2}]_{\text{cyt},T} \approx 9$ mM) exceeds the buffering capacity by as much as fivefold. As a result, the right-hand term of Eq. (10) is a direct measure of the total number of Ca^{2+} ions moved. Equating this term to Eq. (8) gives:

$$\Delta[Ca^{2+}]_{\text{cyt},T} = \Delta[\text{rhod2-Ca}]_{\text{cyt},T} \cdot K_P \approx \Delta[\text{quin2-Ca}]_{\text{cyt},T} \tag{11}$$

and hence

$$K_P \approx \frac{\Delta[\text{quin2-Ca}]_{\text{cyt},T}}{\Delta[\text{rhod2-Ca}]_{\text{cyt},T}}. \tag{12}$$

In Eq. (12), both the numerator and denominator of the right-hand term can be easily evaluated from the following parallel equations:

$$\Delta[\text{quin2-Ca}]_{\text{cyt},T} = \Delta\alpha \cdot [\text{quin2}]_{\text{cyt},T} \tag{13}$$

$$\Delta[\text{rhod2-Ca}]_{\text{cyt},T} = \Delta\alpha_1 \cdot [\text{rhod2}]_{\text{cyt},T} \tag{14}$$

where $\Delta\alpha$ and $\Delta\alpha_1$ represent the differences in degrees of quin2 and rhod2 complexation, respectively, each determined at the beginning and end of the linear rise in fluorescence (*cf.* left-hand side of Fig. 3). The value of K_P, thus calculated, was found to be 8.6, and the total number of Ca^{2+} ions moved was determined from the relation:

$$\Delta[Ca^{2+}]_{\text{cyt},T} = 8.6 \cdot \Delta[\text{rhod2-Ca}]_{\text{cyt},T}. \tag{15}$$

Knowledge of the value of K_P also allows determination of the value of k_{iono}, the proportionality constant between ionomycin concentration and the rate of Ca^{2+} influx (*cf.* Eq. (6)). Division of both sides of Eq. (8) by the duration of the linear phase of Ca^{2+} influx, (Δt) makes the left-hand terms of Eqs. (6) and (8) equal. Solving for k_{iono} then yields the following equation:

$$k_{\text{iono}} = \frac{K_P \cdot (\Delta[\text{rhod2-Ca}]_{\text{cyt},T}/\Delta t)}{[Ca^{2+}]_o \cdot [\text{ionomycin}]}. \tag{16}$$

The second term in the numerator is evaluated from Eq. (14) and Δt. Since K_P, and both terms in the numerator of Eq. (16) are known, k_{iono} is determined (i.e., 19 μM/min).

Application of the Calibration Procedure to Determine Absolute Rates of Ca^{2+} Extrusion

Figure 3 (right-hand side) also compares the progress curves of Ca^{2+} extrusion (Method II) in rhod2-laden *vs.* quin2-overloaded platelets. The comparison shows that the apparent rate of Ca^{2+} extrusion is much faster in rhod2-laden platelets than in quin2-overloaded platelets. In rhod2-laden platelets the half time for completion of the extrusion process is independent of $[\text{rhod2}]_{\text{cyt}}$.

It was previously mentioned that progress curves of Ca^{2+} extrusion were initially analyzed by determining the rates of Ca^{2+} removal from the rhod2 complex, ($-d\alpha_1/dt$; *cf.* Eq. (5)). It will now be shown that these can be converted into absolute rates of extrusion, $V_{\text{extrusion}}$ ($= -d[Ca^{2+}]/dt$, expressed as millimole Ca^{2+} moved per liter cell volume per minute) through the use of an equation (Eq. (18)) which will be derived below.

Substitution of Eq. (14) into Eq. (8), gives:

$$\Delta[Ca^{2+}]_{\text{cyt},T} = \Delta\alpha_1 \cdot [\text{rhod2}]_{\text{cyt},T} \cdot K_P. \tag{17}$$

Multiplication of both sides of Eq. (17) by $-(1/\Delta t)$ and its expression in differential notation then yields:

$$V_{\text{extrusion}} = (-d[Ca^{2+}]_{\text{cyt},T})/dt = (-d\alpha_1/dt) \cdot [\text{rhod2}]_{\text{cyt},T} \cdot K_P. \tag{18}$$

Since the use of K_P as a proportionality constant is valid for values of $[Ca^{2+}]_{\text{cyt}}$ (or α_1) falling within the linear range of Ca^{2+} influx, it was important to determine how far this linear range extends. Figure 4 shows an experiment where the linear phase of Ca^{2+} influx can be seen to extend to a value of about 3 μM for $[Ca^{2+}]_{\text{cyt}}$. Extension of linearity to higher values of $[Ca^{2+}]_{\text{cyt}}$ required increasing the ionomycin concentration to 2.5 μM and removing external Na^{2+} to stop the Na^+/Ca^{2+} exchanger.

Characterization of Cytoplasmic Ca^{2+} Buffering Capacity with Rhod2

Figure 5 (solid curve) shows the Ca^{2+} dependence of cytoplasmic buffering capacity determined in the present study. This determination is based on the previously described calibration procedure which evaluates the proportionality constant K_P (*cf.* Eqs. (8)–(12) and Figs. 3 and 4). Knowledge of K_P in Eq. (9) determines $\Delta[B\text{-Ca}]_T$, the additional cytoplasmic buffering capacity complexed to Ca^{2+}. Upon rearranging Eq. (9), one obtains the following equation for $\Delta[B\text{-Ca}]_T$:

$$\Delta[B\text{-Ca}]_T = (K_P - 1) \cdot \Delta[\text{rhod2-Ca}]_{\text{cyt},T} = \Delta[\text{quin2-Ca}]_{\text{cyt},T} - \Delta[\text{rhod2-Ca}]_{\text{cyt},T}. \tag{19}$$

To use Eq. (19), it only need be shown that the values of $[Ca^{2+}]_{\text{cyt}}$ corresponding to the upper and lower limits of $\Delta[\text{rhod2-Ca}]_{\text{cyst},T}$ fall within the linear range of Ca^{2+} influx. This range has been shown to be extend to values as high as 2.7 μM (*cf.* Fig. 4). In the latter experiment the value of K_P was 10.2 in the range of 0.1 to 2.7 μM $[Ca^{2+}]_{\text{cyt}}$.

The results in Fig. 5 were obtained after addition of the contribution made by previously characterized buffering capacity (Johansson & Haynes, 1988) at 0.12 μM $[Ca^{2+}]_{\text{cyt}}$. In the present study the buffering capacity at $[Ca^{2+}]_{\text{cyt}} \leq 2.7$ μM shows a more linear dependence of the binding phenomena on $[Ca^{2+}]_{\text{cyt}}$ than was previously revealed by quin2 (Johansson & Haynes, 1988). The concentration of binding sites is 3.6 mM in the range of $[Ca^{2+}]_{\text{cyt}} = 0.1$–$2.7$ μM and their apparent $K_d = 0.87$ μM.

Ionomycin Short-Circuit Method (Method II)

The basis for this method is as follows: In the presence of external Ca^{2+} low concentrations of ionomycin, which do not overwhelm the capacity of the plasmalemmal extrusion mechanisms, are

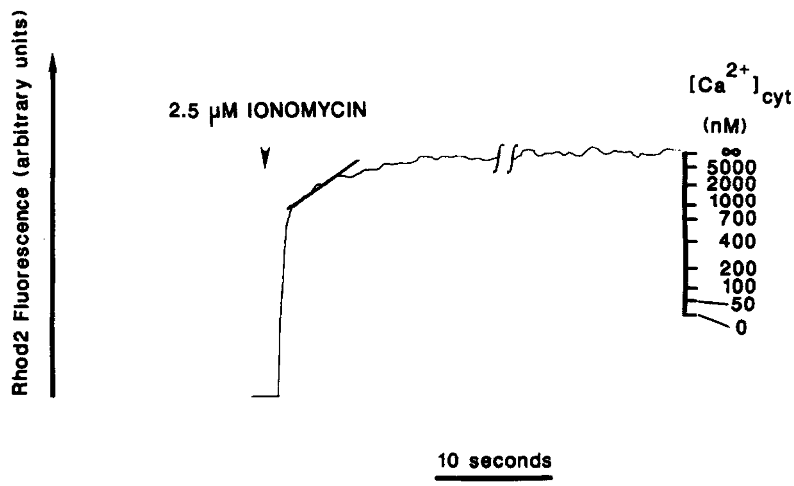

Fig. 4. Progress curve of ionomycin-mediated Ca^{2+} influx ($NMDG^+$ Tyrode) showing extension of linearity to 3 μM $[Ca^{2+}]_{cyt}$. The scale on the left shows the values of $[Ca^{2+}]_{cyt}$. In this experiment $[rhod2]_{cyt}$ = 0.54 mM. Much of the initial rise in fluorescence was missed since it could not be recorded soon enough after the ionomycin addition. (*See* legend to Fig. 3 for details about vertical traces, their initial curvature and timing of the ionomycin addition.) At the time of ionomycin addition $[Ca^{2+}]_o$ was 2.0 mM.

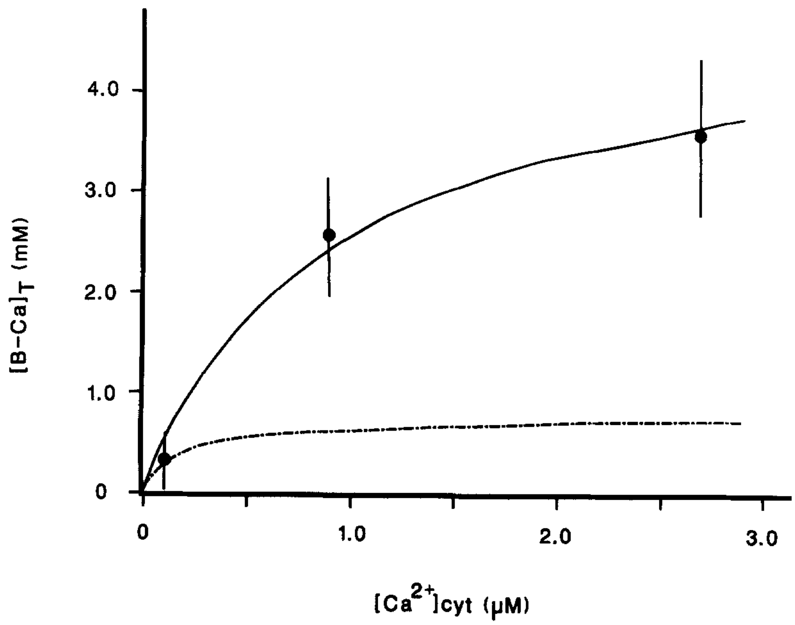

Fig. 5. Dependence of total cytoplasmic Ca^{2+} buffering capacity ($[B\text{-Ca}]_T$) on $[Ca^{2+}]_{cyt}$. The solid line represents the cytoplasmic buffer capacity determined by the method shown in Fig. 3. The absence of curvature in the initial segment of the Ca^{2+} influx curve (*cf.* Fig. 3) is an indication of a linear buffer capacity (*cf.* Materials and Methods, Eq. (19)). Figure 5 is based on a composite of data obtained from experiments shown in Figs. 3*A* and 4. The dashed line represents the contribution by previously characterized binding sites (K_d = 0.14 μM and $[B]_T$ = 0.73 mM; Johansson & Haynes, 1988). The solid curve conforms to the equation:

$$[B\text{-Ca}]_T = \frac{[B]_T \cdot [Ca^{2+}]_{cyt}}{K_d + [Ca^{2+}]_{cyt}}$$

with K_d = 0.87 μM and $[B]_T$ = 4.8 mM.

used to establish different steady-state values of $[Ca^{2+}]_{cyt}$. As predicted by Eq. (6) for the steady-state condition, the unidirectional ionomycin-mediated rate of Ca^{2+} influx plus the passive inward leakage rate is equal to $V_{extrusion}$, the rate of Ca^{2+} extrusion. (At steady state the rate of Ca^{2+} influx ($d[Ca^{2+}]_{cyt,T})/dt$ is equal to zero). Thus, the ionomycin concentration provides a linear measure of the extrusion rate at the various steady-state values of $[Ca^{2+}]_{cyt}$.

Figure 6 illustrates the ionomycin short-circuit method in a typical experiment. The manipulations shown in Fig. 2 for the net extrusion protocol are repeated except that low and varied concentrations of ionomycin are added to the platelets in the presence of 2 mM Ca^{2+}. The low ionomycin levels result in varying degrees of Ca^{2+} influx, which increase $[Ca^{2+}]_{cyt}$ until a steady or quasi-steady state is achieved. To obtain the Ca^{2+} dependence of the absolute rates, the $[Ca^{2+}]_{cyt}$ at the steady state or quasi-steady state is determined. Knowledge of k_{iono} (determined in an earlier subsection; *cf.* Eq. (16)) allows conversion of the lower ionomycin concentrations into absolute initial rates of Ca^{2+} influx. To these, the previously determined contribution of passive inward leakage observed in the absence of ionomycin (Johansson & Haynes, 1988) is added and the rates are plotted as a function of $[Ca^{2+}]_{cyt}$.

Experimentation Using CTC as a Probe for Dense Tubular Ca^{2+}

The use of CTC to monitor dense tubular Ca^{2+} has also been previously described (Jy & Haynes, 1984; Johansson & Haynes, 1988). As in the latter study, it was used as a control to demonstrate the effectiveness of 1 μM ionomycin in short circuiting dense tubular Ca^{2+} uptake while the extrusion processes were being monitored. This was done to rule out dense tabular Ca^{2+}

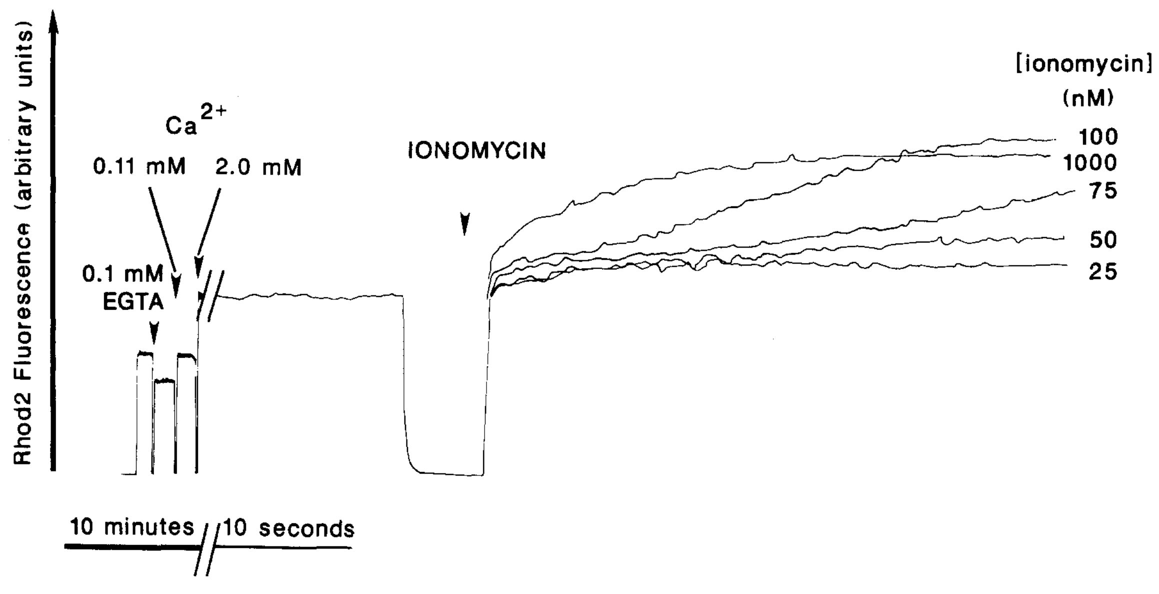

Fig. 6. Protocol used in the ionomycin short-circuit method (Method II). Details of the method are given in the text. Each trace of increasing fluorescence has been corrected for changes in baseline and has been scaled by a factor (1.17–2.03) to correct for different degrees of dye loss at the onset of the experiment and at steady state, respectively. The scaling factor increases with increasing ionomycin concentration.

uptake as a mechanism contributing to the clearance of cytoplasmic Ca^{2+} during the extrusion process.

Curve Fitting Statistics

Curve fitting and statistics were done using ASYSTANT (Macmillan Software). The one-tailed Student's *t* test for paired variables was carried out with the aid of EPISTAT (copyright Tracy L. Gustafson).

Results

Kinetics of Ca^{2+} Extrusion Determined by the Ca^{2+} Extrusion Protocol (Method I)

Figure 7 shows a typical pair of traces from experiments demonstrating the Na^+ dependence of the extrusion process. In the presence of external Na^+, 75% of the extrusion process is over in 45 sec. In the absence of external Na^+, it takes 2.5 min before α_1 attains a value of 0.25 (25% saturation). The faster Ca^{2+} extrusion rate reflects activity of both the plasmalemmal Ca^{2+}-ATPase and the Na^+/Ca^2 exchanger, whereas the slower Ca^{2+} extrusion rate reflects the activity of the Ca^{2+}-ATPase alone.

The traces in Fig. 7 were analyzed to obtain the Ca^{2+} dependence of the rates of Ca^{2+} removal. The analysis was done as follows: The slopes ($-dF/dt$) of each progress curve of decreasing fluorescence were determined for values of $[Ca^{2+}]_{cyt}$ given by the scale on the left-hand side of the figure. The slopes, which represent absolute rates of fluorescence decrease, were then converted into rates of Ca^{2+} removal from the rhod2-Ca complex ($-d\alpha_1/dt$; *cf.* Materials and Methods, Eq. (5). In regard to conversion of $-d\alpha_1/dt$ into absolute rates (*cf.* Eq. (18)), we have previously shown that the change in rhod2 fluorescence is proportional to $\Delta[Ca^{2+}]_{cyt,T}$, the total number of Ca^{2+} ions moved. This was shown to be true in the range of 0.1–3 μM $[Ca^{2+}]_{cyt}$ (*cf.* Materials and Methods, Fig. 4). Figure 8 plots rate *vs.* $[Ca^{2+}]_{cyt}$. In the figure the rates ($-d\alpha_1/dt$) are presented as a fraction of the highest rate observed in the presence of Na^+ ($[Ca^{2+}]_{cyt}$ = 8.3 μM). Figure 8*A* shows the Ca^{2+} dependence of the rates of Ca^{2+} removal from rhod2 measured both in the presence and absence of external Na^+. Figure 8*B* presents the difference between the two curves, which is the contribution of the exchanger. The contribution of the exchanger is roughly half that of the pump. Over the range of 0.1–3 μM $[Ca^{2+}]_{cyt}$, the rates of extrusion shown in Fig. 8*A* (Na^+ curve) can be shown to conform to the following equation:

$$V_{\text{extrusion}} = \frac{V_{\max,1} \cdot [Ca^{2+}]_{cyt}^{1.7}}{K_{m,1}^{1.7} + [Ca^{2+}]_{cyt}^{1.7}} + \frac{V_{\max,2} \cdot [Ca^{2+}]_{cyt}}{K_{m,2} + [Ca^{2+}]_{cyt}} \quad (20)$$

where the first term with parameters subscripted

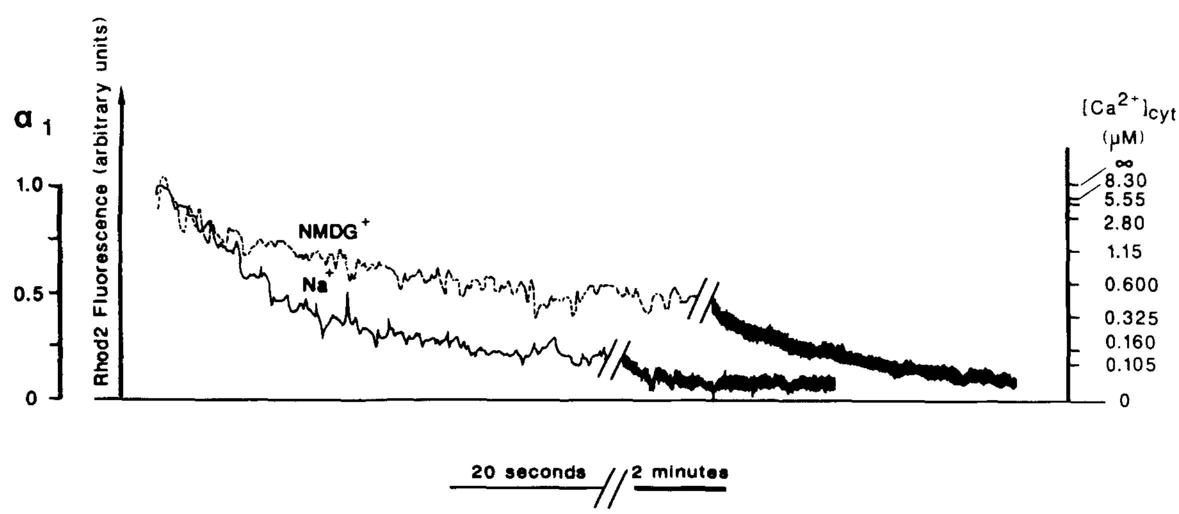

Fig. 7. Typical experiment showing progress curves for active Ca^{2+} extrusion in the presence and absence of Na^+. The curves are labeled by the predominant extracellular cation and represent plots of α_1 (*cf.* Eq. (4)) *vs.* time. The nonlinear scale on the right shows values of $[Ca^{2+}]_{cyt}$ at which the absolute rates of extrusion were determined. The curve obtained with $NMDG^+$ has been corrected for a 24% loss of high-affinity dye (and hence loss in fluorescence change). In the presence of $NMDG^+$ the dye loss is reproducibly greater than in the presence of Na^+. If the correction had not been applied, the difference between control and experimental curves would have been larger.

with 1 refers to the Ca^{2+}-ATPase (as determined by Johansson & Haynes, 1988). A good fit was obtained with a Hill coefficient of 1.7. The second term with parameters subscripted with 2 refers to the rate of the Na^+/Ca^+ exchanger.

The Table summarizes the values of the best fit parameters. It shows that the Na^+/Ca^{2+} exchanger has a $K_m = 0.95 \pm 0.27$ and a $V_{max} = 0.96 \pm 0.56$ mM/min. The apparent K_m of the Ca^{2+} pump is 0.72 ± 0.06 μM and the $V_{max} = 1.3 \pm 0.5$ mM/min. The apparent K_m and the V_{max} of the Ca^{2+}-ATPase are 10 to 20-fold as large as previously published (Johansson & Haynes, 1988). Results below will give evidence that the higher and more prolonged elevation of $[Ca^{2+}]_{cyt}$ incurred by this protocol is responsible for these changes.

Confirmation that 1 μM Ionomycin Is Sufficient to Short Circuit Dense Tubular Ca^{2+} Uptake

Chlortetracycline fluorescence is a linear measure of free $[Ca^{2+}]$ in the dense tubules (Jy & Haynes, 1984; Johansson & Haynes, 1988). Figure 9 shows typical CTC experiments performed under conditions identical to those performed with rhod2-laden platelets in Figs. 2 and 7. Figure 9*A* shows the results of EGTA addition in the absence of 1 μM ionomycin. In the absence of ionomycin very little Ca^{2+} is taken up by the dense tubules during the "calcium phase" and there is little to leak during the "EGTA phase." In the presence of ionomycin and with elevation of $[Ca^{2+}]_{cyt}$, some Ca^{2+} is taken up during the "Ca^{2+} phase." It is released in the first 10 sec of the "EGTA phase," and there is no further change thereafter. Thus the dense tubules cannot influence $[Ca^{2+}]_{cyt}$ for the times greater than 10 sec after EGTA addition.

Characterization of Ca^{2+} Extrusion Kinetics by the Ionomycin Short-Circuit Method (Method II)

This method is based on addition of low ionomycin concentrations which set Ca^{2+} influx into competition with the Ca^{2+} extrusion systems, such that a stable elevated value of $[Ca^{2+}]_{cyt}$ is reached when the two competing processes achieve steady state. Figure 10*A* and *B* show the Ca^{2+} dependence of the rate of Ca^{2+} extrusion obtained by the ionomycin short-circuit method. Figure 10*A* shows dependence of steady-state $[Ca^{2+}]_{cyt}$ on ionomycin concentration (*x*- and *y*-axes are in the reverse of convention). Figure 10*B* shows the same data with ionomycin concentrations converted into absolute rates of influx (= rates of extrusion; *cf.* Materials and Methods). The solid curve (pump plus exchanger in the

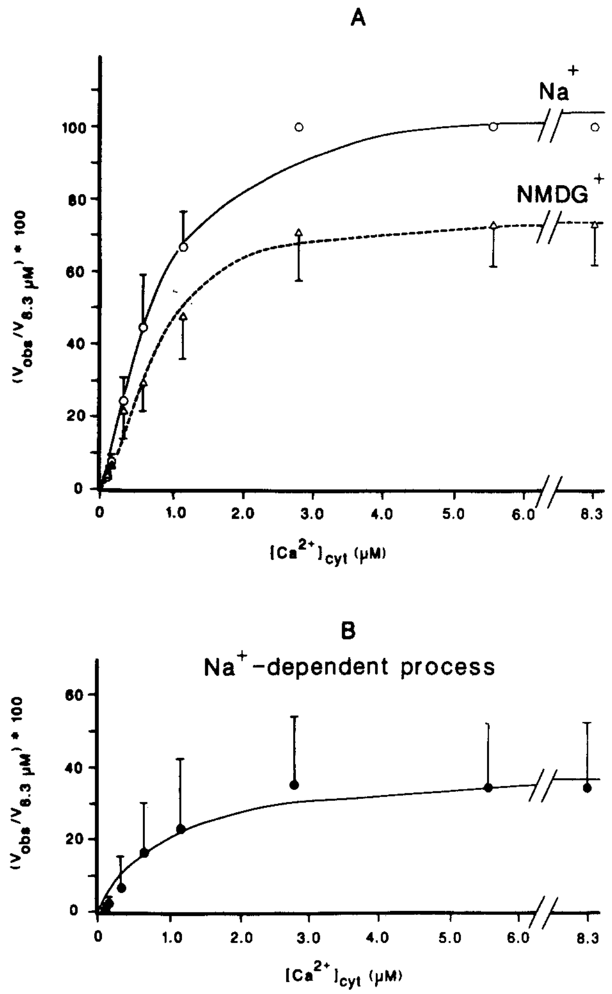

Fig. 8. The $[Ca^{2+}]_{cyt}$ dependence of rates of Ca^{2+} extrusion (removal from rhod2-Ca) in the presence and absence of external Na^+. (*A*) Open circles represent the presence of Na^+ (Ca^{2+}-ATPase and the Na^+/Ca^{2+} exchanger); open triangles represent the absence of Na^+ ($NMDG^+$). (*B*) Filled circles represent the difference between the two curves shown in *A* (contribution of the Na^+/Ca^{2+} exchanger). The experiment of Fig. 7 was repeated five times, and the rates obtained in the presence Na^+ and $NMDG^+$ were analyzed pairwise. The data are presented as observed rate, V_{obs} ($= -d\alpha_1/dt$; *see* Materials and Methods), divided by the highest rate measured in the presence of Na^+, $V_{8.3\ \mu M}$. The average value of $V_{8.3\ \mu M}$ was 1.08 ± 0.42 units of α_1 per min. The data shown represent the means ± SE. Differences between mean values of rate (in Na^+ *vs.* in $NMDG^+$ medium) were statistically significant ($P < 0.05$) at the following values of $[Ca^{2+}]_{cyt}$: 2.8, 5.55 and 8.3 μM.

Table. Summary of values for kinetic parameters for Ca^{2+} extrusion systems

	Pump			Exchanger	
Method/ (condition)	$V_{max,1}$ (mM/min)	$K_{m,1}$ (μM)	Hill coefficient	$V_{max,2}$ (mM/min)	$K_{m,2}$ (μM)
Method I (basal)	1.3 ± 0.5 (0.098)[a]	0.72 ± 0.06 (0.08 μM)[a]	1.7 (1.7)[a]	0.96 ± 0.56	0.95 ± 0.27
Method II	1.9 ± 0.2	0.38 ± 0.06	4.4	1.1 ± 0.4	1.0 ± 0.6

[a] Johansson and Haynes, 1988.

The pump parameters for the exchanger determined by Methods I and II are defined in Eqs. (20) and (21), respectively. The pump parameters determined by Method II (*cf.* Fig. 10*A* and *B*) were fitted to the following equation:

$$V = \frac{(0.098\ \text{mM/min}) \cdot [Ca^{2+}]_{cyt}^{1.7}}{0.08\ \mu M^{1.7} + [Ca^{2+}]_{cyt}^{1.7}} + \frac{V_{max,1} \cdot [Ca^{2+}]_{cyt}^{n}}{K_{m,1}^{n} + [Ca^{2+}]_{cyt}^{n}}$$

with the best fit value of $n = 4.4$. The values of the observed rates, $V_{extrusion}$ are given by:

$$V_{extrusion} = -(d\alpha_1/dt) \cdot [\text{rhod2}]_{cyt} \cdot K_P$$

(*cf.* Materials and Methods, Eq. (18)). All values are expressed as the mean ± SD ($n = 5$).

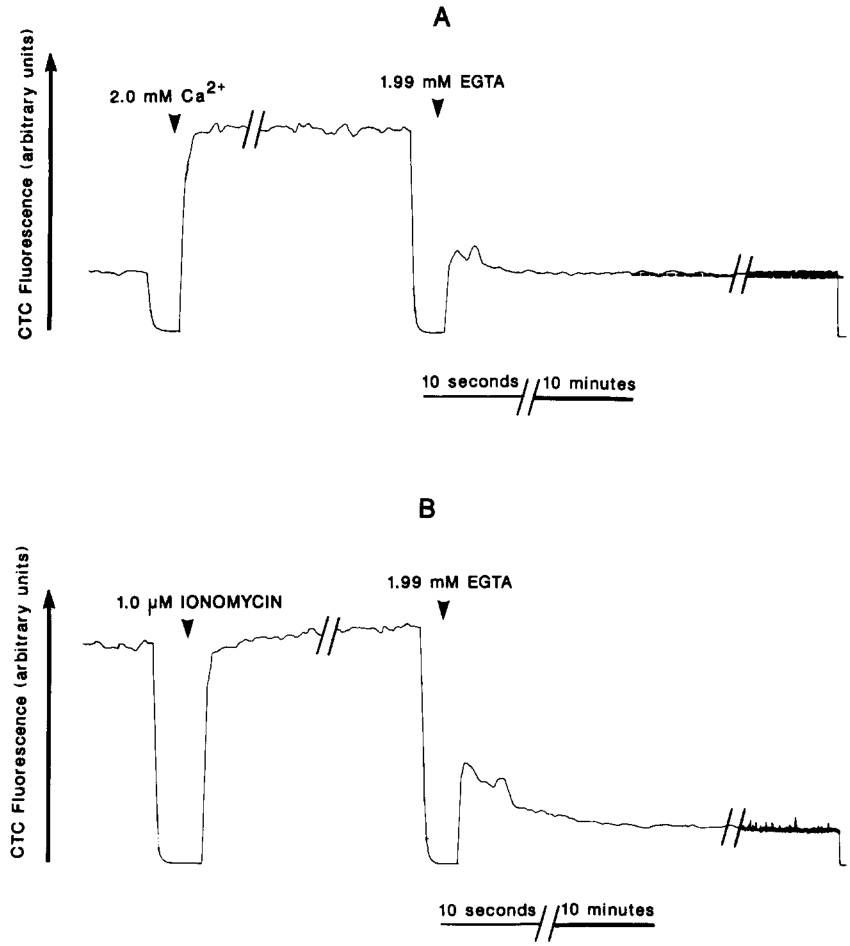

Fig. 9. Chlortetracycline experiments showing minimal changes in dense tubular Ca^{2+} for the net extrusion protocol. (*A*) CTC fluorescence as described in the text (*cf.* Results; Jy & Haynes, 1984; Johansson & Haynes, 1988). (*B*) The effect of 1 μM ionomycin. Following the addition of ionomycin (which increases dense tubular uptake in the presence of external Ca^{2+}) and EGTA, the instantaneous drop in fluorescence is followed by a time-resolved decrease in fluorescence which flattens without any subsequent increase. (*A*: Platelet exposure to 2 mM Ca^{2+} lasted 50 sec. *B*: Platelet exposure to 2 mM Ca^{2+} plus ionomycin lasted 58 sec.) The second break in each of the two traces does not denote a time lapse but a transition from a faster to a slower time scale.

presence of Na^+) represents the best fit of the extrusion data to the following equation (Fig. 10*B*):

$$V_{\text{extrusion}} = \overset{\text{(Basal Pump)}}{\frac{(0.098\ \text{mM/min}) \cdot [Ca^{2+}]_{\text{cyt}}^{1.7}}{0.08\ \mu\text{M}^{1.7} + [Ca^{2+}]_{\text{cyt}}^{1.7}}} + \overset{\text{(Pump)}}{\frac{V_{\max,1} \cdot [Ca^{2+}]_{\text{cyt}}^{4.4}}{K_{m,1}^{4.4} + [Ca^{2+}]_{\text{cyt}}^{4.4}}} + \overset{\text{(Exchanger)}}{\frac{V_{\max,2} \cdot [Ca^{2+}]_{\text{cyt}}}{K_{d,2} + [Ca^{2+}]_{\text{cyt}}}}. \qquad (21)$$

The dashed line, which describes the Ca^{2+} pump (in presence of $NMDG^+$), was fitted to Eq. (21) minus the last term for the exchanger. In the second term of Eq. (21), $K_{m,1}$ represents both the K_m of the activated state and the EC_{50} for pump activation. The data shown were obtained from five different platelet preparations. Increased scatter observed at higher ionomycin concentrations occurs because $[Ca^{2+}]_{\text{cyt}}$ is very sensitive to changes in the rate of Ca^{2+} influx.

The Table also summarizes the best fit values of kinetic constants obtained by this method. The Hill coefficient of 4.4 is higher than that of 1.7 obtained by the net extrusion protocol. Otherwise the values of $V_{\max}$ and K_m of the exchanger agree reasonably well with those obtained by the net extrusion protocol.

Reverse Operation of the Exchanger

Figure 11 shows a typical experiment, demonstrating the effect of monensin on the resting $[Ca^{2+}]_{\text{cyt}}$. Monensin catalyzes Na^+/H^+ exchange across the plasma membrane, thus increasing the cytoplasmic Na^+ activity ($[Na^+]_{\text{cyt}}$). The increase in $[Na^+]_{\text{cyt}}$ in turn allows operation of the Na^+/Ca^{2+} exchanger in the reverse mode by shifting the equilibrium in favor of Ca^{2+} influx via the exchanger. As a result, $[Ca^{2+}]_{\text{cyt}}$ in the experiment is increased to 300 nM. At this steady state, the Ca^{2+} pump is working against the exchanger at 90% of its basal value of $V_{\max}$. Considerable variation in the magnitude of the monensin-induced increase in $[Ca^{2+}]_{\text{cyt}}$ was observed in different platelet preparations.

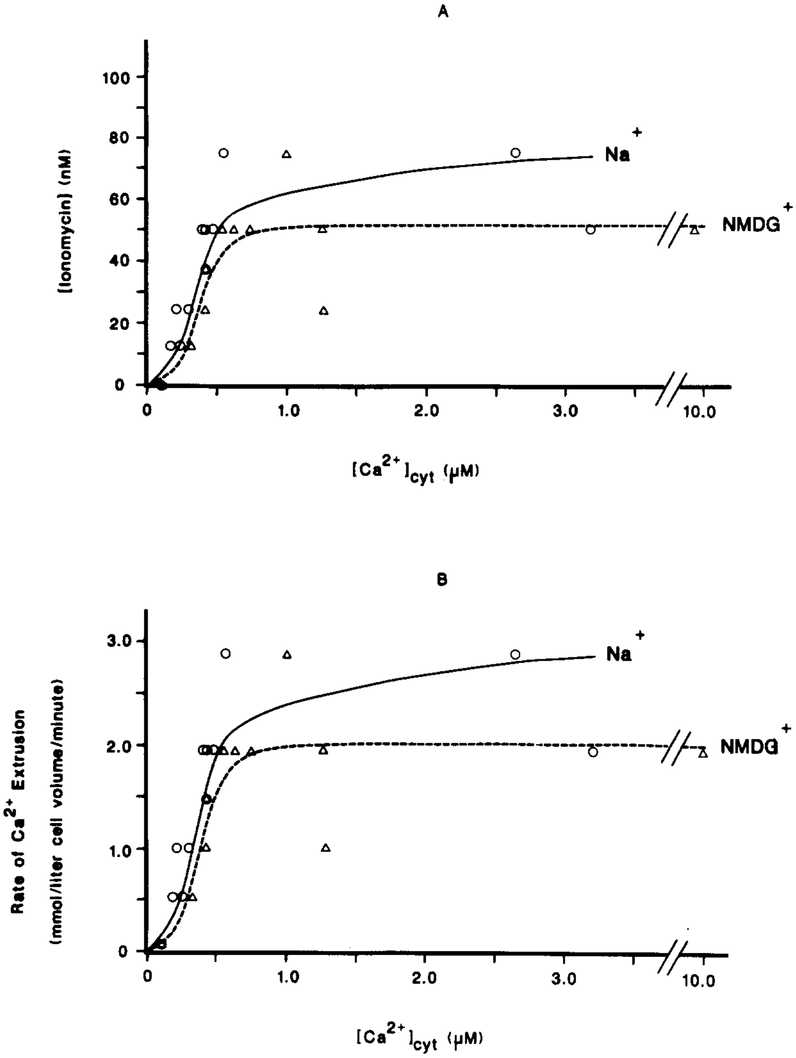

Fig. 10. $[Ca^{2+}]_{cyt}$ dependence of extrusion rates determined by the ionomycin short-circuit method. (*A*) A plot of ionomycin concentration (ordinate) *vs*. steady-state levels of cytoplasmic Ca^{2+} (abscissa). The results shown were obtained in the presence (open circles) and absence of external Na^+ ($NMDG^+$ Tyrode; open triangles). The steady-state $[Ca^{2+}]_{cyt}$ corresponding to zero ionomycin was set at 110 nM. At this $[Ca^{2+}]_{cyt}$, the passive inward Ca^{2+} influx is opposed by the Ca^{2+}-ATPase working at 0.63 times its V_{max} for the basal state (Johansson & Haynes, 1988). (*B*) The ionomycin concentrations shown in *A* have been converted into rates of Ca^{2+} extrusion (mmol/liter cell volume/min). To these was added a small contribution of the (ionomycin-independent) inward passive Ca^{2+} influx which was calculated as $0.63 \cdot V_{max}$ (basal) of the Ca^{2+}-ATPase, as previously determined by Johansson and Haynes (1988). This amounts to 0.062 mmol/liter cell volume/min. Open circles represent the Na^+/Ca^{2+} exchanger and the Ca^{2+}-ATPase; open triangles represent the Ca^{2+}-ATPase.

In addition to increasing $[Na^+]_{cyt}$, monensin causes a cytoplasmic alkalinization of 0.3–0.5 pH unit (P.A. Valant and D.H. Haynes, *unpublished observations*) and might thus increase the sensitivity of quin2 to Ca^{2+}. Therefore, control experiments (*not shown*) were done showing that the above pH change does not significantly alter the quin2 signal. In these experiments platelet cytoplasm was transiently alkalinized by the addition of 25 mM NH_4Cl. The alkalinization was comparable in magnitude to that caused by monensin (P.A. Valant and D.H. Haynes, *unpublished data*). It was found to have no reproducible effect on the quin2 signal.

Discussion

In the present study, the kinetics of Ca^{2+} extrusion by plasmalemmal systems of the intact human platelet were determined over the 1–10-μM range of $[Ca^{2+}]_{cyt}$ values. This characterization was achieved with rhod2 (the high-affinity form), a fluorescent indicator which has a fivefold lower affinity for Ca^{2+} than quin2. Although the commercially available dye was heterogeneous and leaked considerably from platelets into the external medium, difficulties arising from this type of dye behavior were overcome. The major contributions of this study were: (i) The *in situ* characterization of the Ca^{2+} extrusion kinetics of the Na^+/Ca^{2+} exchanger; the latter was shown to saturate and its V_{max} and K_m were determined. (ii) Demonstration that activation of the plasmalemmal Ca^{2+} pump occurs at the higher levels of $[Ca^{2+}]_{cyt}$ (*ca.* 10 μM) attained in rhod2-laden platelets. The activation of the pump is reflected by significant increases in the previously determined values for V_{max}, K_m and possibly the Hill coefficient (Johansson & Haynes, 1988). (iii) The determination of cytoplasmic Ca^{2+} binding capacity at higher values of $[Ca^{2+}]_{cyt}$. The buffering capacity is higher than we

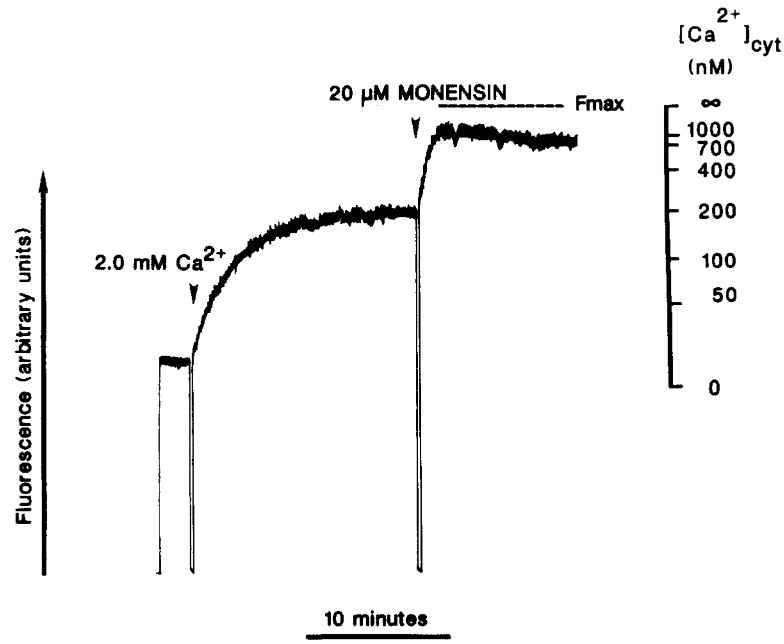

Fig. 11. Monensin causes an increase in resting levels of $[Ca^{2+}]_{cyt}$ in quin2-overloaded platelets. Platelets that had been preincubated with 20 μM quin2 (quin2 overload) were resuspended in Na^+ Tyrode with HCO_3^- at pH 7.4 and 2 mM Ca^{2+} was added. At steady state (resting $[Ca^{2+}]_{cyt}$), 20 μM monensin was added and the maximal increase in fluorescence was measured. Ionomycin (1 μM) was finally added to obtain F_{max}. F_{min} was obtained in parallel experiments in which the platelets were lysed with 40 μM digitonin in the presence of 2 mM EGTA. In the experiment shown, $[Ca^{2+}]_{cyt}$ rose from 192 to 362 nM. The nonlinear scale on the right gives values of $[Ca^{2+}]_{cyt}$.

established before (Johansson & Haynes, 1988) and shows a more linear dependence of Ca^{2+} binding on Ca^{2+} activity in the 0.1- to 3-μM range of $[Ca^{2+}]_{cyt}$. The buffering capacity is also higher than can be accounted for by calmodulin.

Characteristics of the Na^+/Ca^{2+} Exchanger *In Situ*

The contribution of the exchanger was assessed from the difference in rates measured in the presence and absence of external Na^+ ($NMDG^+$ substitution). The Na^+/Ca^{2+} exchanger was found to have a V_{max} of 1.0 ± 0.6 mmol/liter cell volume/min and a K_m of 0.97 ± 0.31 μM. There was good agreement in the results obtained by each of two approaches (the net Ca^{2+} extrusion protocol and the ionomycin short-circuit method). The K_m values obtained in the platelet are in reasonable agreement with those reported for other cell types or preparations (range: 0.2–8 μM). These include cardiac sarcolemmal vesicles (lower limit; Reeves, 1985), the squid optic nerve (Osses, Condrescu & DiPolo, 1986), coated vesicles from the brain (Saermark & Gratzl, 1986), and kidney basolateral membranes (Jayakumar et al., 1984; van Heeswijk, Geersten & van Os, 1984). The ability of the exchanger to operate in reverse was also confirmed. Taken together, these findings further corroborate the existence of a Na^+/Ca^{2+} exchanger in the human platelet.

Physiological Significance of the Na^+/Ca^{2+} Exchanger

The Exchanger as a Check against Accidental Activation

We have shown that the exchanger has a 10-fold greater V_{max} than the pump in its basal state. The physiological role of the exchanger appears to be that of a reserve mechanism for rapid restoration of $[Ca^{2+}]_{cyt}$ from the micromolar range to resting values following platelet activation. The latter may occur accidentally in response to various submaximal stimuli as the platelet circulates in the bloodstream. Since platelet activation becomes an irreversible process, the platelet may require the presence of the exchanger to prevent spurious activation by submaximal stimuli. Thus, the exchanger may have an important role in the system of checks and balances, which determine whether or not platelet activation will occur.

Possible Role of the Exchanger in Platelet Activation

The finding that monensin causes a rapid rise in $[Ca^{2+}]_{cyt}$ demonstrates operation of the exchanger in reverse is in agreement with the initial observations of Rengasamy et al. (1987) on isolated platelet membranes and those of Schaeffer and Blaustein (1989) in intact platelets. Our results indicate the rate of Ca^{2+} influx via the exchanger is comparable to the V_{max} of the Ca^{2+} pump in the basal state.

The above interpretation of the monensin effect is based on control studies showing that alkalinization of the cytoplasm *per se* by NH_4Cl does not cause a change in $[Ca^{2+}]$. The latter results are in contrast to those of Ghigo et al. (1988) who observed a significant increase in $[Ca^{2+}]_{cyt}$ after addition of 20 mM NH_4Cl to quin2-laden platelets. The difference may be explained by the absence of external HCO_3^- in the medium used by Ghigo et al. (1988), since Cl^-/HCO_3^- exchange has been shown to accelerate restoration of cytoplasmic pH after an alkalinizing challenge with NH_4Cl (P.A. Valant & D.H. Haynes, *unpublished observations*).

It is known that thrombin causes platelet activation largely by increasing the rate of Ca^{2+} influx (Rink, Smith & Tsien, 1982*b*). However, recent patch-clamp studies done with platelet membranes indicate that addition of thrombin does not result in channel activation (Mahaut-Smith, Sage & Rink, 1990, 1991). In addition, there is earlier evidence indicating that one of the early events in platelet activation by thrombin is an increased entry of external Na^+ (Horne et al., 1981; Davies, Dunn & Simmons, 1987; Siffert & Akkerman, 1987; Siffert et al., 1989; Borin & Siffert, 1990). This raises the possibility that the Na^+ entry precedes Ca^{2+} influx and induces the latter by raising $[Na^+]_{cyt}$ sufficiently to reverse the operation of the exchanger. Among the possible mechanisms responsible for the thrombin-induced increase in Na^+ influx are activation of the Na^+/H^+ exchanger by a transient cytoplasmic acidification (Zavoico et al., 1986) and activation of a Na^+ channel. The elucidation of the sequence of events involved in thrombin activation would be worthy of future study in light of the possible participation of the Na^+/Ca^{2+} exchanger.

HIGH $[Ca^{2+}]_{cyt}$ ACTIVATES THE PUMP

The present study has given evidence for activation of the plasmalemmal Ca^{2+}-ATPase by high $[Ca^{2+}]_{cyt}$. In the activated state the observed pump V_{max} and the K_m are 10- to 20-fold greater than those determined previously for the pump in the basal state (Johansson & Haynes, 1988). Pump activation may have a similar role to that of the exchanger, i.e., protection against platelet activation by marginal stimuli. Preliminary experiments (*not shown*) done with 1 μM calmidazolium, a calmodulin inhibitor, indicate that it inhibits pump activation. This suggests that the activation is mediated by a Ca-calmodulin (Ca-CAM)-dependent process.

For pump activation to become evident, it is necessary to subject platelets for critical periods of time to high levels of $[Ca^{2+}]_{cyt}$. In the present experimentation with rhod2-laden platelets, the platelet cytoplasm has been subjected to elevations of $[Ca^{2+}]_{cyt} \geq 10$ μM for durations as long as 15–60 sec. The activation process appears to be maximal at values of $[Ca^{2+}]_{cyt} \geq 1$ μM.

The results obtained by the net Ca^{2+} extrusion protocol and the ionomycin short-circuit method are in good agreement with respect to values of the pump K_m and V_{max}. However, the Hill coefficient obtained by the first method is 1.7, while that obtained by the second method is 4.4 (compare Eq. (20) with Eq. (21)). The difference in Hill coefficients can be explained as follows: When the Ca^{2+} extrusion protocol is used, all the platelet samples are exposed to very high levels of Ca^{2+}. Under these conditions it is likely that all platelet samples attain the same maximal state of activation by Ca-CAM. Thus, the apparent K_m value of 0.72 μM is the one associated with full pump activation. However, when the ionomycin short-circuit method is used, only the platelet samples exposed to high ionomycin concentrations and high $[Ca^{2+}]_{cyt}$ attain full activation. Samples exposed to lower ionomycin concentrations undergo partial or no activation. The apparent K_m of 0.38 μM may also reflect the EC_{50} for the activation process, which is intermediate between the K_m for the basal state (0.08 μM) and the K_m for the fully activated state (0.72 μM). The fourth power dependence on $[Ca^{2+}]_{cyt}$ with the ionomycin short-circuit method may thus reflect the process of saturation of calmodulin (CAM) with Ca^{2+}.

Ca-calmodulin-dependent activation of the Ca^{2+}-ATPase has been previously demonstrated in plasmalemmal vesicles of the bovine heart (Caroni & Carafoli, 1981; Dixon & Haynes, 1989). Dixon and Haynes (1989) observed a 9- to 12-fold increase in V_{max}, which is in good agreement with the results obtained in the present study. Ca-calmodulin also increased the Hill coefficient (1.7 basal *vs.* 3.7 with Ca-CAM). However, CAM-dependent activation in cardiac sarcolemmal vesicles increased the apparent Ca^{2+} affinity 28-fold. This is in contrast to our present findings, which show that pump activation in the platelet is associated with a 6- to 10-fold increase in apparent K_m.

In the study with cardiac sarcolemmal vesicles (Dixon & Haynes, 1989), activation of the pump by cAMP-dependent protein kinase increased the V_{max} by only a factor of two. This agrees with recent findings showing that dibutyryl cAMP and forskolin (which increases cAMP levels) increase the V_{max} (basal) of the pump roughly by a factor of two (Johansson et al., 1992). It is therefore unlikely that CAM-dependent adenylate cyclase accounts for the large increase in V_{max} during pump activation in the platelet.

Further characterization of the pump activation process and the specificity of the calmidazolium effect will be addressed in a future publication. It would also be useful to study the pump in isolated vesicles, where CAM could be better manipulated as was previously done for the bovine heart (Dixon & Haynes, 1989).

Respective Contributions of the Na^+/Ca^{2+} Exchanger and the Ca^{2+} Pump

In the basal state, the plasmalemmal Ca^{2+} pump has a K_m of 80 nM and a V_{max} of 0.098 mM/min (Johansson & Haynes, 1988). As a result, the Ca^{2+} pump has a high sensitivity to small elevations of free Ca^{2+} in the 50- to 400-nM range of $[Ca^{2+}]_{cyt}$. Its principal function in the basal state is to maintain the resting level of $[Ca^{2+}]_{cyt}$ by opposing the effects of passive inward leakage of Ca^{2+} across the cell membrane. The latter amounts to 63% of the V_{max} of the pump at the resting value of $[Ca^{2+}]_{cyt}$ of 110 nM (Johansson & Haynes, 1988). In contrast, the Na^+/Ca^{2+} exchanger has a K_m of about 1 μM and a V_{max} which is 10-fold higher than that of the pump in the basal state. Hence, for increments in $[Ca^{2+}]_{cyt} \geq 400$ nM, the initial response of the exchanger can rapidly restore $[Ca^{2+}]_{cyt}$ towards resting values. If $[Ca^{2+}]_{cyt}$ still continues to remain high, pump activation within seconds provides an additional mechanism for rapid restoration of resting $[Ca^{2+}]_{cyt}$ from high levels. The pump V_{max} increases at the expense of a higher K_m for Ca^{2+}, but the latter change would not be of consequence when the Ca^{2+} pump works at $[Ca^{2+}]_{cyt} \geq 900$ nM. Together, the exchanger and pump activation may protect the circulating platelet from accidental activation by inappropriate or marginal stimuli.

We thank Mr. William Watzek for expert assistance and Mr. Alan Mandveno for advice in word processing. This work was supported by U.S. Public Health Service HL38228, HL07188 and the Florida Heart Association.

References

Borin, M., Siffert, W. 1990. Stimulation by thrombin increase the cytosolic free Na^+ concentration in human platelets. *J. Biol. Chem.* **265:**19543–19550

Brand, L., Witholt, B. 1967. Fluorescence Measurements. *In:* Methods in Enzymology. C.H.W. Hirs, editor. Vol. 11, pp. 809–813. Academic, New York.

Caroni, P., Carafoli, E. 1981. The Ca^{2+}-pumping ATPase of heart sarcolemma. Characterization, calmodulin dependence and partial purification. *J. Biol. Chem.* **256:**3263–3270

Davies, T.A., Dunn, J.M., Simmons, E.R. 1987. Evaluation of changes in cytoplasmic pH in thrombin-stimulated human platelets. *Anal. Biochem.* **167:**118–123

Dixon, D.A., Haynes, D.H. 1989. Kinetic characterization of the Ca^{2+}-pumping ATPase of the cardiac sarcolemma in four states of activation. *J. Biol. Chem.* **264:**13612–13622

Fabiato, A. 1979. Calculator programs for computing the composition of the solutions containing multiple metals and ligands used for experiments in skinned muscle cells. *J. Physiol. (Paris)* **75:**463–505

Fabiato, A. 1981. Myoplasmic free calcium concentrations reached during the twitch of an intact isolated cardiac cell and during calcium-induced release of calcium from the sarcoplasmic reticulum of a skinned cardiac cell from the adult rat or rabbit ventricle. *J. Gen. Physiol.* **78:**457–497

Fabiato, A. 1985. Time and calcium dependence of activation and inactivation of calcium-induced release of calcium from the sarcoplasmic reticulum of a skinned canine cardiac Purkinje cell. *J. Gen. Physiol.* **85:**247–289

Ghigo, D., Treves, S., Turrini, F., Pannocchia, A., Pescarmona, G., Bosia, A. 1988. Role of Na^+/H^+ exchange in thrombin- and arachidonic acid-induced Ca^{2+} influx in platelets. *Biochim. Biophys. Acta* **940:**141–148

Horne, W.C., Norman, N.E., Schwarz, D.B., Simons, E.R. 1981. Changes in cytoplasmic pH and in membrane potential in thrombin stimulated human platelets. *Eur. J. Biochem.* **120:**295–302

Jayakumar, A. Cheng, L., Liang, C.T., Sacktor, B. 1984. Sodium gradient-dependent calcium uptake in renal basolateral membrane vesicles. *J. Biol. Chem.* **259:**10827–10833

Johansson, J.S. 1990. Characterization of the Ca^{2+} Extrusion Systems of Human Platelets. Ph.D. Dissertation. University of Miami, Miami (FL)

Johansson, J.S., Haynes, D.H. 1988. Deliberate quin2 overload as a method for *in situ* characterization of active calcium extrusion systems and cytoplasmic calcium binding: Application to the human platelet. *J. Membrane Biol.* **104:**147–163

Johansson, J.S., Haynes, D.H. 1992. Cyclic GMP increases the rate of the calcium extrusion pump in intact human platelets but has no direct effect on the dense tubular calcium accumulation system. *Biochim. Biophys. Acta* **1105:**40–50

Johansson, J.S., Neid, L.E., Haynes, D.H. 1992. Cyclic AMP stimulates Ca^{2+}-ATPase mediated Ca^{2+} extrusion from human platelets. *Biochim. Biophys. Acta* **1105:**19–28

Jy, W., Ahn, Y.S., Shanbaky, N., Fernandez, L.F., Harrington, W.J., Haynes, D.H. 1987. Abnormal calcium handling by platelets in thrombotic disorders. *Circ. Res.* **60:**346–355

Jy, W., Haynes, D.H. 1984. Intracellular calcium storage and release in the human platelet: Chlortetracycline as a continuous monitor. *Circ. Res.* **55:**595–608

Jy, W., Haynes, D.H. 1987. Thrombin-induced calcium movements in platelet activation. *Biochim. Biophys. Acta* **929:**88–102

Jy, W., Haynes, D.H. 1988. Calcium uptake and release characteristics of dense tubules of digitonin-permeabilized human platelets. *Biochim. Biophys. Acta* **944:**374–382

Mahaut-Smith, M.P., Sage, S.O. Rink, T.J. 1990. Receptor-activated single channels in intact human platelets. *J. Biol. Chem.* **265:**10479–10483

Mahaut-Smith, M.P., Sage, S.O., Rink, T.J. 1991. ADP, but not thrombin, rapidly activates cation channels in human platelets. *Biophys. J.* **59:**374*a*

Minta, A., Kao, J., Tsien, R. 1989. Fluorescent indicators for

cytosolic calcium based on rhodamine and fluorescein chromophores. *J. Biol. Chem.* **264**:8171–8178
Osses, L., Condrescu, M., DiPolo, R. 1986. ATP-dependent calcium pump and Na-Ca exchange in plasma membrane vesicles from squid optic nerve. *Biochim. Biophys. Acta* **860**:583–591
Reeves, J.P. 1985. The sarcolemmal sodium-calcium exchange system. *Curr. Top. Membr. Transp.* **25**:77–127
Rengasamy, A., Soura, S. Feinberg, H. 1987. Evidence for Na^{+}-Ca^{2+} exchange in platelet plasma membranes. *Thromb. Haemost.* **57**:337–340
Rink, T.J., Smith, S.W., Tsien, R.Y. 1982*b*. Cytoplasmic free Ca^{2+} in human platelets: Ca^{2+} thresholds and Ca-independent activation for shape change and secretion. *FEBS Lett.* **148**:21–26
Rink, T.J., Tsien, R.Y., Pozzan, T. 1982*a*. Cytoplasmic pH and free Mg^{2+} in lymphocytes. *J. Cell Biol.* **95**:189–196
Saermark, T., Gratzl, M. 1986. Na-Ca exchange in coated microvesicles. *Biochem. J.* **233**:643–648
Schaeffer, J., Blaustein, M.P. 1989. Platelet free calcium concentrations measured with fura-2 are influenced by the transmembrane sodium gradient. *Cell Calcium* **10**:101–113
Siffert, W., Akkerman, J.W.N. 1987. Activation of sodium-proton exchange modulates Ca^{2+} mobilization in human platelets. *Nature* **325**:456–458
Siffert, W., Siffert, G., Scheid, P., Akkerman, J.W.N. 1989. Activation of Na^{+}/Ca^{2+} exchange and Ca^{2+} mobilization start simultaneously in thrombin-stimulated platelets. *Biochem. J.* **258**:521–527
Tsien, R.Y., Pozzan, T., Rink, T.J. 1982. Calcium homeostasis in intact lymphocytes: Cytoplasmic free calcium monitored with a new, intracellularly trapped fluorescent indicator. *J. Cell Biol.* **94**:325–334
van Heeswijk, M.P.E., Geersten, J.A.M., van Os, C.N. 1984. Kinetic properties of the ATP-dependent Ca^{2+} pump and the Na^{+}-Ca^{2+} exchanger in basolateral membranes of the rat kidney cortex. *J. Membrane Biol.* **79**:19–31
Ware, J.A., Smith, M., Fossel, E.T., Salzman, E.W. 1988. Cytoplasmic Mg^{2+} concentration in platelets: Implications for determination of Ca^{2+} with aequorin. *Am. J. Physiol.* **255**:H855–H859
Zavoico, G.B., Cragoe, E.J., Feinstein, M.B. 1986. Regulation of intracellular pH in human platelets. Effects of thrombin A23187, and ionomycin and evidence for activation of Na^{+}/H^{+} exchange and its inhibition by amiloride analogues. *J. Biol. Chem.* **261**:13160–13167

Received 21 February 1992; revised 1 May 1992

Appendix A

Characteristics of Rhod2 as a Ca^{2+} Indicator

Ca^{2+} titrations of rhod2 were done to characterize form of the signal dependence on Ca^{2+} activity. An aliquot of rhod2 (free acid) was introduced into Na^{+} Tyrode (nominally Ca^{2+} free). This was followed by addition of 2.0 mM EGTA. The sample was then titrated with increasing concentrations of Ca^{2+} to construct curves of fluorescence *versus p*Ca. Values of *p*Ca were calculated using stability constants obtained from Alexandre Fabiato-Computer Programs (Fabiato, 1979, 1981, 1985).

Figure A1 shows a typical Ca^{2+} titration curve obtained in vitro with a sample of the free-acid form of rhod2. The shape of the curve indicates the presence of two titratable groups, one saturating at a Ca^{2+} activity of 10 μM (the high-affinity form) and the other saturating at 5 mM Ca^{2+} (the low-affinity form). Figure A2 shows that similar results were obtained under the same conditions with digitonin lysate of EGTA-treated platelets previously loaded with rhod2/AM. Platelets were either left intact or lysed with 40 μM digitonin after the EGTA addition prior to titration with Ca^{2+}. The K_d values of dye obtained from platelet lysate agree with those obtained with the free acid, but the latter shows a greater contribution to fluorescence by the high-affinity dye. The results can be described by Eq. (2) (*cf.* Materials and Methods).

Table A1 shows that the K_d values of the products of rhod2/

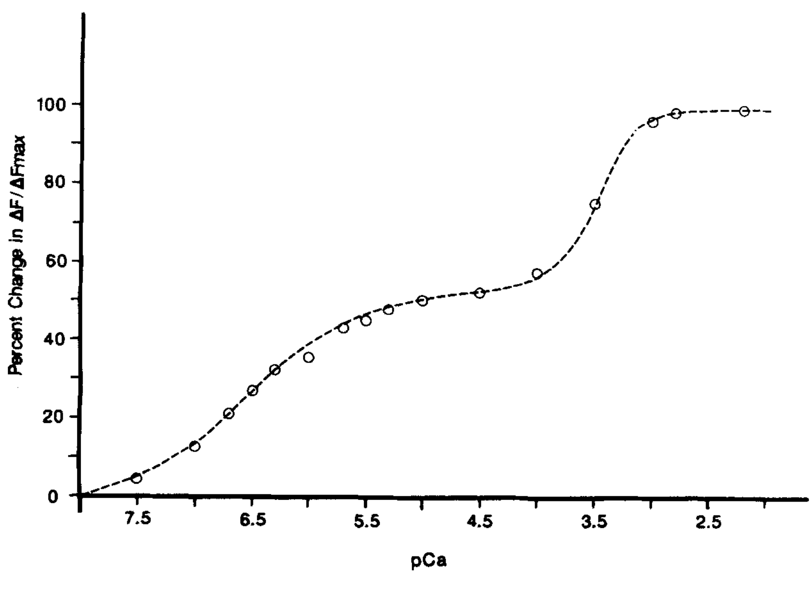

Fig. A1. Ca^{2+} titration of 0.2 μM rhod2-free acid in Na^{+} Tyrode solution at pH 7.25 (0 Mg^{2+}). The $[Ca^{2+}]/[EGTA]$ ratio was varied between 0.263 and 6.00. The total [EGTA] was 1.96 mM.

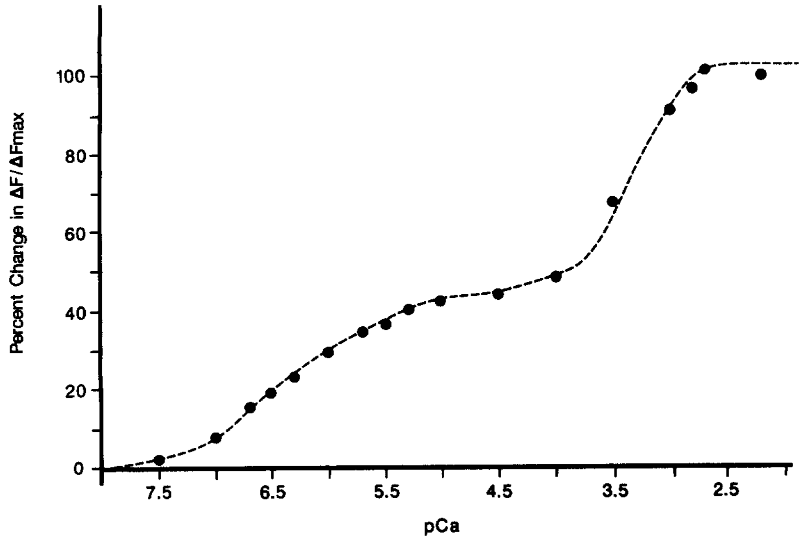

Fig. A2. Ca^{2+} titration of product of rhod2/AM hydrolysis after platelet lysis in Na^+ Tyrode at pH 7.25 (0 Mg^{2+}). Other conditions are described in the legend to Fig. A1.

Table A1. Characteristics of high- and low-affinity forms of rhod2

	High affinity		Low affinity		
Form	% Contribution (X_1)	K_d (nM)	% Contribution ($1 - X_1$)	K_d (μM)	% F_{min}/F_{max}
Free acid	40.6 ± 5.8	383 ± 19	59.4 ± 5.8	1195 ± 111	29.3 ± 1.7
Leaked dye (before manipulations)	17.9 ± 3.2	352 ± 89	82.1 ± 3.2	1130 ± 114	—
Product of rhod2/AM (lysate)	21.9 ± 8.7	361 ± 139	78.1 ± 8.7	1262 ± 136	11.0 ± 0.7
Cytosolic before lysis	20.5 ± 4.5	—	79.5 ± 4.5	—	—
Cytosolic released upon lysis	17.2 ± 6.1	—	82.8 ± 6.1	—	—

Titration of rhod2-free acid (0.2 or 0.5 μM) was performed in Na^+ Tyrode at pH 7.25, after addition of 2 mM EGTA. Following addition of 2 mM EGTA, the Ca^{2+} titration was also performed on leaked dye with the rhod2-laden platelets remaining intact or on dye released after platelet lysis with 40 μM digitonin. The results shown in the last two rows compare the $(F_{max} - F_{min})_{cyt}$ values from progress curves of decreasing fluorescence (*cf.* Fig. 2) with the fluorescence change resulting from the release of high-affinity dye from previously intact platelets into a medium containing 10 μM free Ca^{2+}. The release was induced by digitonin lysis of Ca^{2+}-depleted platelets. These platelets had been exposed to 2 mM EGTA prior to their lysis in the presence of 10 μM $[Ca^{2+}]_o$. All the above values represent means ± SD ($n \geq 2$). Dashes (—) represent undetermined values.

AM hydrolysis and the free form of the dye in vitro do not differ significantly. It also shows that 40 μM digitonin does not alter the K_d of either form of the dye. Table A1 does not reveal large differences in leakage of the two forms of the dye.

In vitro titrations of different lots of the dye (free-acid form) have shown different proportions of low- and high-affinity form. For example, with an earlier lot (lot number 8B) of rhod2, the proportion of high-affinity form (X_1; *cf.* Eq. (2) in Materials and Methods) was 55 ± 7.0% ($n = 4$) to the total fluorescence under a given set of conditions. In a later lot (lot number 10A) X_1 was 79 ± 7.1% ($n = 4$).

HPLC Analysis of Rhod2

HPLC was performed on a reverse phase Whatman C-18 column attached to a composite Beckmann HPLC system, with a model 165 variable-wavelength detector. Figure A3 shows a typical chromatogram. At least five different peaks can be reproducibly resolved, indicating the presence of at least three components in the original sample. The peaks elute between 13.4 and 25.6 min after injection. The retention time corresponds to the passage of about 20 void volumes. Our finding of several major components in the commercially supplied product is sufficient to explain the presence of two affinities for Ca^{2+}

These results are in contrast to those given by the supplier who provided the following information (Paul R. Johnson, *personal communication*): In the supplier's assay a single peak eluted 5.5 min after injection. Their column was described a reverse phase C-2, from Brownlee, packed with SiO_2 with a 5–μM particle size. The void volume, though unknown, was estimated as $\frac{1}{6}$th of its volume (4.16 ml) or 0.692 ml. The supplier's procedure was to ramp the initial mobile phase (40% ACN plus 60% TFA) to 100% ACN in 30 min and hold at 100% for 5 min. The flow rate was

Table A2. In vitro effects of pH and Mg^{2+} on the relative contribution to total fluorescence and on the K_d of each form of rhod2-free acid

		High affinity		Low affinity	
pH	$[Mg^{2+}]$ (mM)	% Contribution (X_1)	K_d (nM)	% Contribution ($1 - X_1$)	K_d (μM)
7.05	0	41.2 ± 3.2	354 ± 10	58.8 ± 3.2	634 ± 182
7.05	0.10	50.7 ± 7.9	358 ± 132	49.3 ± 7.9	227 ± 116
7.05	1.0	38.3 ± 7.7	651 ± 6	61.7 ± 7.7	504 ± 207
6.78	0	68.0 ± 5.3	753 ± 15	32.0 ± 5.3	291 ± 130
6.78	0.10	86.8 ± 8.9	997 ± 24	12.2 ± 8.9	599 ± 173
6.62[a]	0	75.6 ± 0.6	945 ± 67	24.4 ± 0.6	250 ± 70
6.62[a]	1.0	73.8 ± 0.2	910 ± 3	26.2 ± 0.2	217 ± 26

Rhod2-free acid (0.5 μM) was introduced into a high K^+ (155–160 mM K^+) and low Na^+ (15–20 mM) medium buffered with 50 mM HEPES. Following addition of 2 mM EGTA to reduce the external Ca^{2+} concentration to zero, the dye was titrated with increasing concentrations of Ca^{2+}. *p*Ca values were determined as described in Materials and Methods. The titration curves were fitted by computer to obtain best fit values of K_d and relative fluorescence. The above values represent the mean ± SD.

[a] Titration was performed as above with 0.1 μM rhod2 in the presence of 150 mM PIPES and 15 mM Na^+ at about the same ionic strength (i.e., 210 mM K^+). All titrations were done at 37°C.

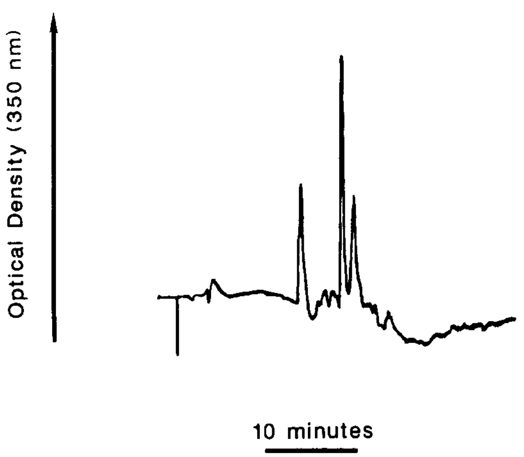

Fig. A3. A typical chromatogram of rhod2 obtained by HPLC. A 2.0-mM aqueous solution of rhod2 was diluted 50-fold in a mixture of 40% acetonitrile (ACN) and 60% trifluoroacetic acid (TFA; 0.2% in water). The diluted rhod2 was filtered through a 22-μm filter prior to loading onto the HPLC column. An aliquot of 25 μl (0.8 μg of dye) was loaded onto the column. The mobile phase was a mixture of 20% ACN and 80% TFA. Following injection of the sample, the mobile phase was ramped to 100% ACN over a period of 20 min and held at 100% for 6 min. The flow rate was 0.7–0.75 ml/min. The void volume of the column was 0.5 ml. The contents of the eluate were monitored at wavelengths of 254 and 350 nm.

given as 1.0 ml/min with monitoring at 254 and 556 nm. From the flow rate, we could estimate that about eight volumes passed through the C-2 column before elution of the single peak. These considerations indicate that the latter column had a 2.5-fold lower retention time than the C-18 column used in the present study. The resulting difference in resolving power would be sufficient to explain the discrepancy between our results and those of the supplier.

pH and Mg^{2+} Dependence of Rhod2 Fluorescence

Table A2 summarizes the results of further characterization of the two forms of rhod2 in terms of their apparent K_d for Ca^{2+} and in terms of their contribution to total fluorescence in the presence of saturating levels of free Ca^{2+}, respectively. These were determined at pH 7.05 both in the absence and presence of 0.1 and 1.0 mM Mg^{2+}. The literature reports values of free cytosolic Mg^{2+} concentrations ranging from 0.25 to 1.0 mM (Rink et al., 1982*a*; Ware et al., 1988). Given that the K_d varies between 350 and 950 nM over this range of Mg^{2+} concentrations, an average apparent K_d of 500 nM was used in all calculations of cytoplasmic Ca^{2+} activity.

Ca^{2+}-Insensitive Form of Rhod2

Table A1 also shows that values of F_{min} obtained within platelet lysate are 30% of the total F_{max}. Values of F_{min} obtained with the free form in vitro are 11%. This difference can be explained by release of a Ca^{2+}-insensitive quenched form of rhod2 that is present in intact platelets. This form of dye behaves as if its fluorescence were self-quenched by its accumulation in the hydrophobic bilayer of cell membranes. It is evidenced by a digitonin-lysis-induced increase in fluorescence (amounting to about 20% of the total ΔF_{max}) in zero external Ca^{2+} (18 mM EGTA), even under conditions of moderate dye loading (preincubation with 12 μM rhod2/AM). Increasing the preincubation concentration of rhod2/AM increases the proportion of this Ca^{2+}-insensitive form of the dye. Disruption of cell membranes by either digitonin or exposure to high Ca^{2+} and/or ionomycin increases the release of this form into the external medium where dye dilution removes self-

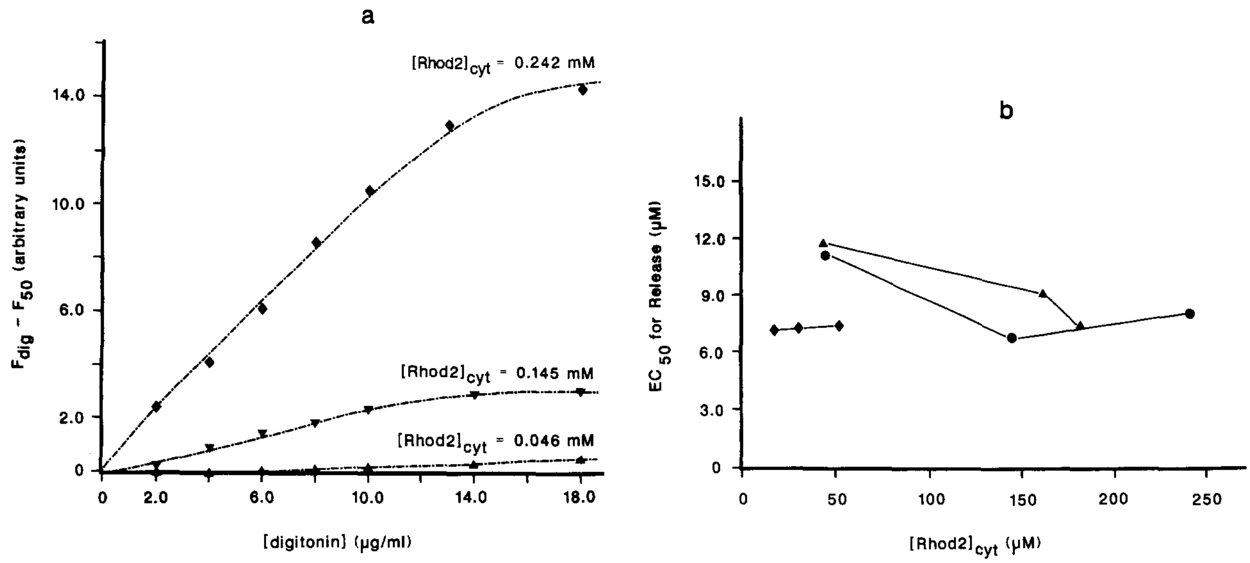

Fig. A4. (*a*) Example of the cumulative increase in fluorescence as a function of digitonin concentration for platelets preincubated with 3, 12 and 24 μM rhod2/AM. The concentration of digitonin was increased in small increments following flattening of the progress curve of decreasing fluorescence at the end of the extrusion protocol shown in Fig. 2. The $[Ca^{2+}]_o$ was 10 μM. The ordinate represents the digitonin-induced increase in fluorescence with respect to F_{50} of the progress curve. The abscissa represents the corresponding concentration of digitonin. The same procedure was repeated for each degree of dye loading. At the highest $[rhod2]_{cyt}$, the change in fluorescence upon full release of the dye is much greater than one would predict from the increase in cytoplasmic dye concentration. This effect can be explained by self-quenching of fluorescence in the cytoplasm at higher values of $[rhod2]_{cyt}$ (Brand & Witholt, 1967). (*b*) The plot of EC_{50} for the digitonin-induced rise in fluorescence *vs*. rhod2 loading for three different preparations. The values are obtained from Fig. A4*a* (for preincubations with 3, 12 and 24 μM rhod2/AM). The EC_{50} is defined as the concentration of digitonin resulting in half-maximal release of the dye. The results from each preparation are denoted by a different set of symbols.

quenching (Brand & Witholt, 1967). The dye probably is unhydrolyzed rhod2/AM.

Additional Controls for Localization of Rhod2 in Cytoplasmic Compartment

Experiments were done to eliminate the possibility that rhod2 is accumulated in a noncytoplasmic intracellular compartment. Platelets were subjected to three different degrees of loading (preincubation with 3, 12 and 24 μM rhod2/AM) and subjected to graded digitonin lysis (Jy & Haynes, 1988) at the end of an efflux protocol. If two or more intracellular compartments had accumulated the dye, a plot of the change in fluorescence *vs*. cumulative digitonin concentration would reveal a bi- or polyphasic pattern of increase in fluorescence, each phase having a different EC_{50} for release. Figure A4*a* is a typical experiment showing that the pattern of fluorescence increase is monophasic. Figure A4*b* shows that the EC_{50} for digitonin-mediated release does not change significantly with increasing intracellular levels of rhod2. Its absolute value is higher than that previously observed for releasing quin2 from the cytoplasmic compartment but is well below the EC_{50} for releasing Ca^{2+} from the dense tubular compartment.